Evolution of earthquake processes

V. V. Ivanov

Institute of Marine Geology and Geophysics, Far East Branch of the Academy of Sciences of the USSR, Sakhalin Island

(Submitted June 18, 1990; resubmitted after revision November 2, 1990)
Usp. Fiz. Nauk **161**, 31–68 (March 1991)

Seismic radiation released during the planar rupture of a glass plate is studied. It is found that this process is complicated: the rupture plane is formed from a sequence of quasilinear cracks running parallel to the initial groove cut in the plate. A quasilinear crack forms with high (seismic) velocity (10^4–10^5 cm/s); the rupture plane, which is built up from a sequence of linear cracks, grows with a low velocity of the order of 10^2–10^3 cm/s. Signals corresponding to the formation of a planar rupture built up from a sequence of linear cracks were found in the spatial and temporal structure of the aftershocks of an Alaskan earthquake. After the signals are interpreted, the earthquake process can be represented as the stagewise formation of several planar ruptures. Each rupture is formed in two phases: During the first phase (lasting 15 min) a leader crack is formed and during the second phase (lasting about one hour) a planar rupture is formed with the leader crack acting as the generatrix. The relationship between the characteristics of the process of successive formation of rupture planes and the parameters of tsunamis generated by the earthquake is analyzed. The relationship between the tsunami focus and the parameters—the coordinates and propagating velocity of the leader crack at the first phase—is established. It is found that the generation time of the high-frequency component is related with the formation of the rupture plane while the generation time of the low-frequency component is related with the successive stages during which successive rupture planes are formed. The possibilities for improving tsunami and earthquake warnings on the basis of the new possibilities for interpretation of seismic signals are discussed.

1. INTRODUCTION

A rule for interpretation of the aftershocks of an earthquake is developed on the basis of analysis of the seismic radiation released during the formation of a planar rupture accompanying the breaking of a glass plate.

This rule is employed together with the methods developed in the last few decades for analyzing signals containing a large number of oscillations to investigate the evolution of an earthquake during the first few hours after the main shock. A correlation is established between the rupture formation process and the characteristics of tsunami generation and the appearance of residual strains accompanying the earthquake. The data obtained from observations of the March 28, 1964 earthquake in Prince William Sound in Alaska are used.

Earthquakes are complicated and varied physical phenomena.[1] They quite often occur in seismically active regions, in some cases causing enormous damage and loss of life. The largest earthquakes (Kamchatka—November 4, 1952; Chile—May 20, 1960; and Alaska—March 28, 1964) are manifested over the entire earth as oscillations of the earth's surface with periods of several seconds and propagate as waves with velocities of several kilometers per second. Seaquakes cause inundations along the coasts of oceans and some seas. These inundations can last for several tens of hours and they propagate along the water surface as waves with periods of about 10 min. For shallow-focus earthquakes the near zone—the focal zone of the earthquake—can be clearly identified. In this zone the manifestations of earthquakes are much more varied. Aside from the above-mentioned seismic vibrations and waves on the surface of water, the following phenomena are also observed: flows of sand and dirt, cracks, fractures, subsidences on the earth's surface, slides, avalanches, motions of cliffs and even mountains, seaquakes (oscillations of the water surface with seismic frequencies), short-wavelength oscillations of the earth's surface with large (1 m) amplitudes, appearance and disappearance of springs, geysers of water and sand, intense and varied sounds, and deformations of the earth's surface.[2] Such phenomena sometimes develop over territories of several thousands of square kilometers and sometimes last for several hours and even days (Figs. 1–4).

Tsunamis and near-zone phenomena of an earthquake are natural disasters and their possibility must be incorporated in civil planning. This involves the construction of barriers, the restriction of building along the coast, the introduction of special insurance regulations, the use of special building designs that take into account the possibility of shaking and deformation of the foundation, and the institution of special networks of stations for organizing warnings for earthquakes and their aftereffects.[3] In the process, for purposes of qualitative assessment earthquakes are represented as an instantaneous point-like process, which is characterized by the epicenter and depth (the spatial coordinate), the time of appearance, and the magnitude (characteristic intensity). On the basis of these quantities the size of the affected region and the magnitude of the tsunami are estimated from the seismograms (records of the vibrations of the earth's surface). Damage is estimated with the help of the concept of the magnitude of the vibrations:

 0038-5670/91/030230-20$01.00

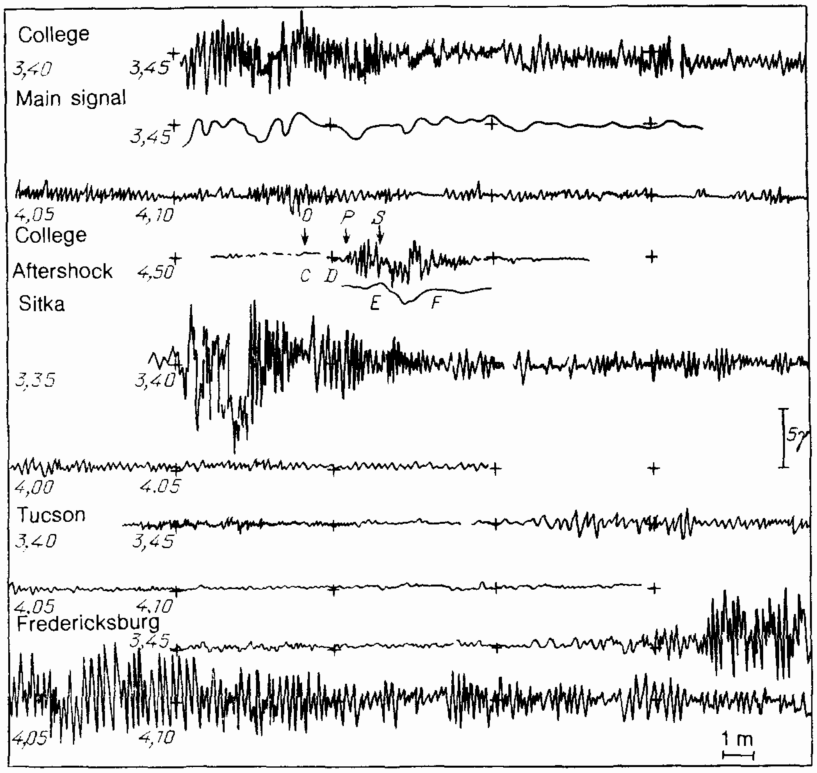

FIG. 1. Seismogram of the March 28, 1964 Alaskan earthquake.

the greater the magnitude, the greater is the damage. For example, magnitude 7 vibrations mean that the earthquake "is felt by everyone, people abandon houses, and well-built houses suffer light damage while poorly built houses suffer heavy damage. In some cases fireplaces and chimneys are destroyed and cars start to move unintentionally from their parking places."[2] The magnitude of the vibrations is calculated based on the distance from the epicenter and the depth and magnitude of the earthquake according to special statistical rules.[4]

Figure 4 shows an example of an actual magnitude map and the results of calculations based on the parameters of the March 28, 1964 earthquake in Alaska. The estimates are based on an interpretation of the parameters of the main shock, which are determined on the basis of the first few minutes of the seismogram.

The relationship between the parameters of the seismic signal and the aftereffects of an earthquake is qualitative. The errors of such a representation can be seen in Fig. 4. The region between the magnitudes 7 and 8 isoseismals contains several points of magnitude 10 and even magnitude 11 vibrations. Moreover, the result of analysis of the observed damage can be represented in the form of simply connected isoseismal lines only for the region of light damage (less than magnitude 7) outside the focal region. Within a single line of magnitudes 7–12 the points with different magnitude are distributed sporadically.[2] In Ref. 2 N. N. Scott and W. K. Cloud note that even at points located at distances of hundreds of kilometers from the epicenter (for the cities of Anchorage and Seward) it is impossible to introduce a single magnitude: the magnitude varies from 10 at one boundary of the city to seven at another boundary. The boundary of the region of complete destruction is clearly seen in aerial photographs of the damaged region of the city of Seward. A general property of the region of destruction can be seen: The region lies in a neighborhood of some line on the surface of the earth. Analysis of the aftereffects of the May 10, 1958 Alaskan earthquake in an uninhabited forested region revealed that the damage (levelling of the trees) occurred in a strip which was several tens of meters wide and hundreds of kilometers long. Near lakes or complicated articulations of geological boundaries (Lituya Bay) the width of the strip increases to several kilometers. Thus the observational data on strong damage is better formalized not as a region but rather as a neighborhood of some lines on the earth's surface which for strong earthquakes form a branched cobweb-like curve that passes through the center of the earthquake. We note that the locations of magnitude 11 vibrations are located, as a rule, in neighborhoods of the branch points of this curve. We shall formulate the first shortcoming of the point-like representation of an earthquake.

Closed, singly connected regions with earthquake vibrations of a definite magnitude represent qualitatively incorrectly the observed pattern of damage. Damage is concentrated in a narrow neighborhood around some line which for strong earthquakes has a complicated structure.

The second significant shortcoming of the existing representation of earthquakes is revealed by an analysis of the real spatial distribution of the times of onset of maximum damage. In the theory of fracture plane formation this is a process of several tens of seconds duration. Its manifestation at different points is delayed by the propagation time of the seismic wave causing the damage. Within the focus this time is no longer than several minutes.[5]

In practice damage is delayed by significantly longer times. The delay at different points in space varies over a

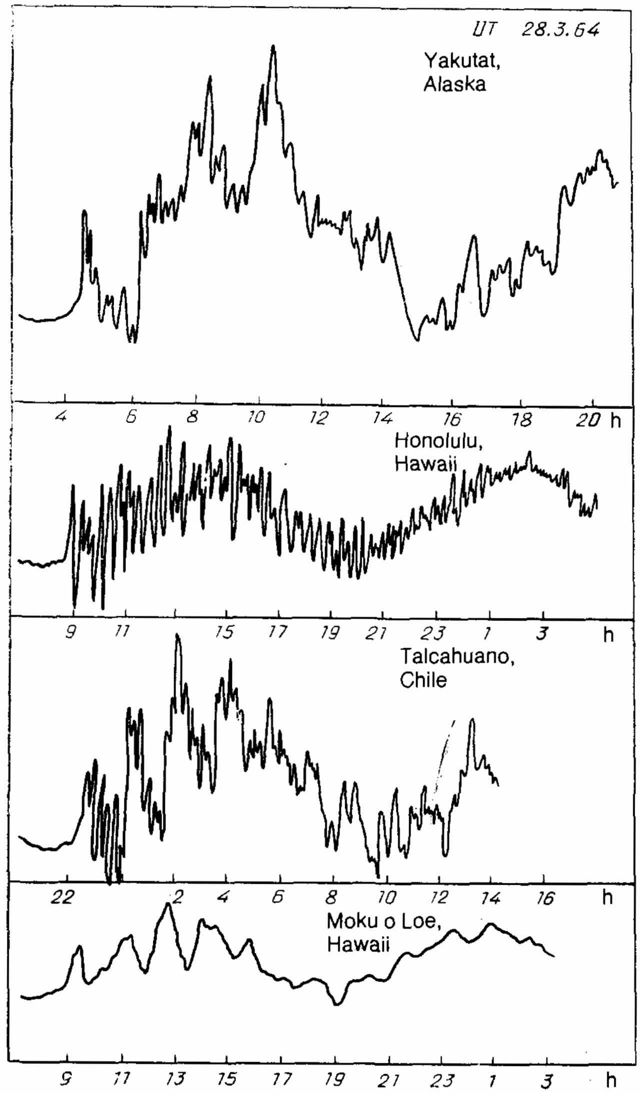

FIG. 2. Records of the tsunami generated by the Alaskan earthquake of March 28, 1964.

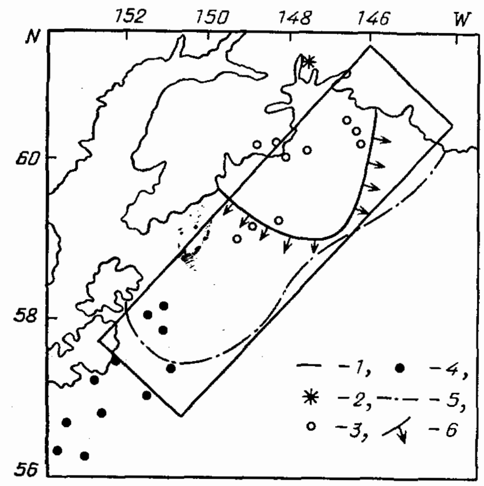

FIG. 3. Map of the focus of the earthquake and tsunami. *1*) Projection of the dislocation plane, *2*) epicenter of the main shock, *3*) epicenters of the southwestern group of aftershocks, *4*) epicenters of the northeastern group of aftershocks, *5*) tsunami wavefront after 15 min, *6*) front of the processes after 3 min.

significant range. Sometimes (March 28, 1964 earthquake in Alaska) it is equal to several minutes and sometimes it is equal to several hours (6 h in Cordova and 8 h in Seldovia).

Thus the description of the delays of the aftereffects of an earthquake creates the impression that the damage-formation process propagates along separate lines in space. Sometimes the damage process rapidly (within several minutes) traverses a distance of hundreds of kilometers along a single line, stops, and then proceeds in a different direction with high velocity. The characteristic times of this complicated process vary from several minutes to several hours. The damage itself does not arise as a result of the maximum accelerations in the seismic wave. Damage is delayed until large-amplitude vibrations of the earth's surface, cracks, and subsidences appear.

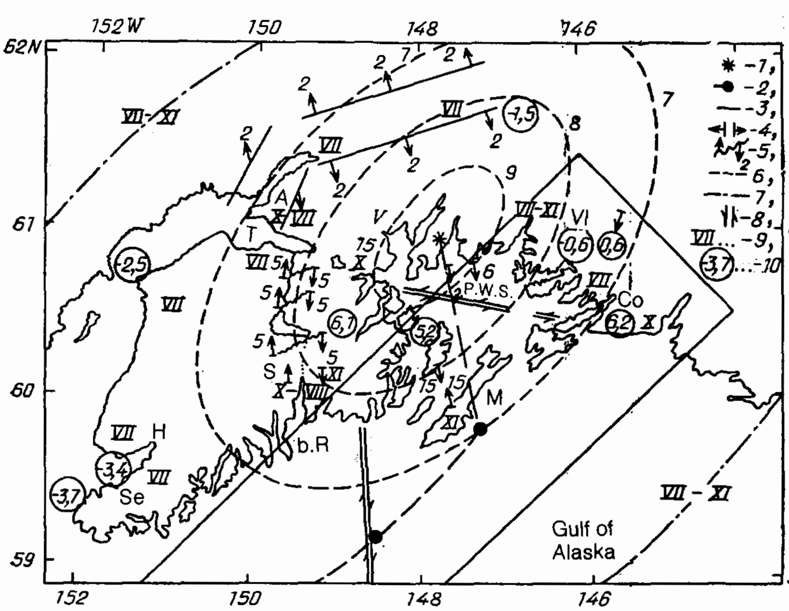

FIG. 4. The near zone of the March 28, 1964 earthquake in Prince William Sound, Alaska. *1*) Epicenter of earthquake, *2*) track of the leader of the first stage, *3*) track of the fault plane, *4*) relative measurements of the displacements, *5*) horizontal displacements (two or more feet; the arrows point in the direction of the displacements), *6*) theoretical magnitude 7 isoseismals, *7*) actual magnitude 7–11 isoseismal, *8*) line of mobile fault, *9*) estimate of the magnitude of the vibrations, *10*) point of measurement of the vertical displacements. A—Anchorage, b. R—Resurrection Bay, VI—Valdez, Co—Cordova, M—Montague Island, P—Portage Island, b. P. W. S.—Prince William Sound, S—Seward, Se—Seldovia, T—Turnagain Arm, H—Homer.

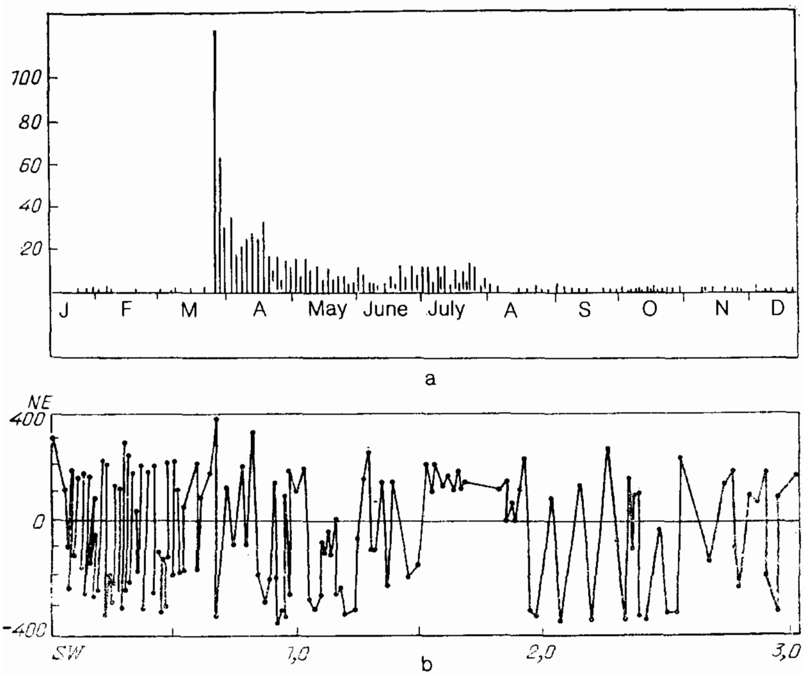

FIG. 5. a) The number of aftershocks per day as a function of time during 1964. b) Displacements of the epicenters of the aftershocks during the first three days after the earthquake.

It must be said that these characteristic time intervals (tens of minutes and hours) are contained in the seismograms (see Figs. 1 and 5) and in the variations of the water level in a tsunami (see Fig. 2). The delays themselves are most clearly determined from the delay of tsunami generation at different locations of the focus.[2] In practical seismology, however, the process is still reduced to a single shock of total duration of several tens of seconds. Separate studies on the analysis of the evolution of the process are now appearing in scientific seismology. These studies are being performed on a different ideological basis:[6-8] They employ different and incompatible representations.

In this review we examine those studies in which the process is represented as a moving source of random seismic vibrations with variable emission intensity. This representation is an extension of the results of Ben-Menachem,[6] who studied a moving "coherent source," and the representation of Wyss and Brune,[9] who were the first to arrive at the conclusion that the first phase of the seismic vibrations is not the only phase that is related with rupture formation. In that distant past (from the scientific standpoint), however, the ideas about the observation and interpretation of a signal described by a nonstationary random process were not yet fully understood,[10,11] so that even these investigations were expanded and extended.[12,13]

The extensions were based on the results of a model experiment.[14] These results are described in Sec. 2. The main result is an extension of the concept of an aftershock. It turns out that an aftershock is not a separate earthquake but rather a maximum of the seismic signal released in a single process of rupture formation, which under real conditions lasts significantly longer than implied by Table I, where statistical estimates of the parameters of the focus of an earthquake are presented. The actual duration sometimes exceeds several hours.

The rupture formation process is by no means isotropic in the rupture plane. It propagates rapidly (with seismic velocities) along a previously formed cut and slowly (with tens and hundreds of times lower velocities) into the sample; in addition, the process propagates into the sample in steps, between which it propagates along the groove cut in the sample. Aftershocks are released whenever the direction of development of the process changes.

The aftershock concept extended in this manner can be employed to construct the trajectory of the emitting point. In Sec. 3 such a representation is constructed for the March

TABLE I. Average parameters of earthquakes.

Magnitude	Seismic moment, dyne·cm	Length of focus, km	Width of focus, km	Magnitude of displacement, cm	Duration, s
1	10^{17}	0,14	0,09	0,003	—
2	$4\cdot10^{19}$	0,4	0,22	0,02	—
3	$1,6\cdot10^{20}$	1,1	0,56	0,1	0,3
4	$6\cdot10^{21}$	3,0	1,4	1,6	1
5	$2,5\cdot10^{23}$	8,3	3,6	3,5	2,5
6	10^{25}	23	9,2	20	7
7	$4\cdot10^{23}$	170	60	120	20
8	$1,6\cdot10^{28}$	170	60	660	60
9	$6\cdot10^{29}$	470	150	3800	150

28, 1964 earthquake in Alaska; the characteristics of the representation are also analyzed in Sec. 3. The main feature is that the rupture surface is formed in a systematic, stagewise fashion.

The relationship between these features and the characteristic manifestations of an earthquake is analyzed in Secs. 4 and 5, including tsunamis (Sec. 5) and characteristic faults along which characteristic movements were produced by the earthquake (Sec. 5).

In order to utilize in practice the new representation of an earthquake the measurements of seismic signals from strong earthquakes must be improved. The questions of measuring seismic signals in order to reconstruct trajectories are studied in Sec. 6.

Thus in this paper we shall study a new representation of earthquakes and the questions of how to organize the measurements and how to use the representation for solving the problems of earthquake warnings.

Some aspects of the earthquake-warning problem, in which progress can be made by using the new representation, are studied in the concluding section (Sec. 7). The scientific problems which are clarified by such a representation of earthquakes are also studied in Sec. 7.

2. MODEL INVESTIGATION OF SEISMIC SIGNALS GENERATED BY THE FRACTURE OF A SOLID BODY

The main physical process that is the source of all manifestations of an earthquake is usually thought to be the formation of a rupture in a solid body. This process has been studied many times. It has important technical applications.[15] However some aspects of this question remain obscure: What determines the rate of formation of the rupture? How is the rupture formed? What signals are released during this process?

The results of special investigations of the temporal evolution of the flux of seismic emissions during the formation of a rupture surface in a glass plate, in which a groove was cut beforehand with a diamond glass cutter, are presented in Ref. 14. The plate was broken in the manner in which this is usually done by glaziers. The special feature of this experiment was that the seismic signals (vertical oscillations of the surface) and strains were recorded. The signals were recorded with the help of piezoelectric sensors attached to the surface of the plate; to record the strains, a strain gauge was attached to the bottom side of the plate.

Samples of window glass with thickness $d = 3$ mm were employed for the experiment. The width of the sample (the rupture length) was varied from 5 to 60 cm. The sample was broken by applying vertical pressure to a horizontal plate (Fig. 6). A groove was cut along the line of the proposed rupture. The force used to break a 20 cm wide plate with a 10 cm arm was equal to approximately 10 kgf. A diagram of the experimental setup is shown in Fig. 6.

Two series of experiments were performed. The purpose of the first series of experiments was to estimate the duration of the rupture formation process. In the second series of experiments the arrangement of the sources of the signal pulses observed in the first series of experiments was investigated.

To estimate the duration of the rupture formation process the moments at which the fracture process started and ended were measured. The moment at which the process started was determined from the record made by the seismic sensor placed on the top surface of the plate 1 cm from the groove. The moment at which the first signal appeared was taken as start of the fracture process. The moment at which the fracture process ends was determined from the record obtained with the strain gauge placed underneath the groove. This moment clearly stood out on the oscillogram as the start of intense variations (Fig. 7).

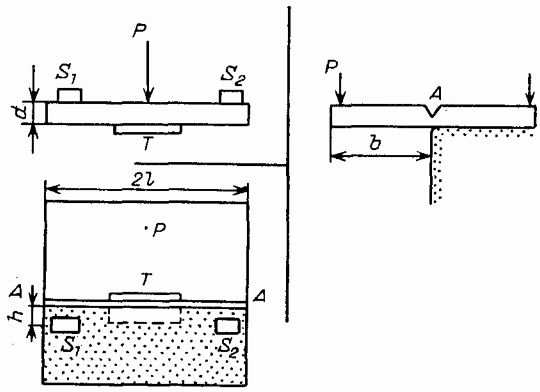

FIG. 6. Diagram of the experiment: the projection of the glass plate, the groove, the sensors, and the loads.

The signals were recorded on an electronic oscillograph, whose sweep rate was chosen so that the entire process from beginning to end was recorded (the timebase is 10 ms/division).

In the second series of experiments the sweep rate was increased up to 0.5 ms/division so that the pulses could be resolved accurately enough to determine their coordinates. As a control, the process was also filmed at a speed of 50 frames/s. But this filming speed was found to be too slow. In rare cases the fracture process was observed in 1–3 frames. As a rule, the process occurred in the period of time between frames.

The most important conclusions follow from the estimated duration T of the rupture formation process. This time interval varied from one experiment to another in the range 5–20 ms. It is much longer than the duration of an individual burst in the seismic signal (10^{-3}–10^{-4} s). About

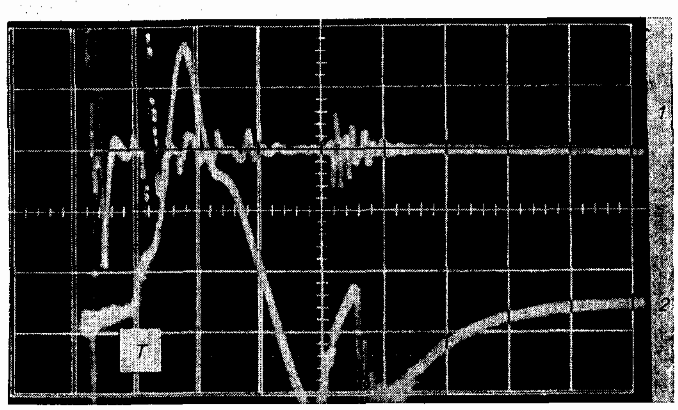

FIG. 7. Record of the signals generated when the plate is broken. The timebase is 10 ms/division. *1*) Seismic signal, *2*) signal from the strain gauge; *T*—the moment at which rupture formation is taken to be completed.

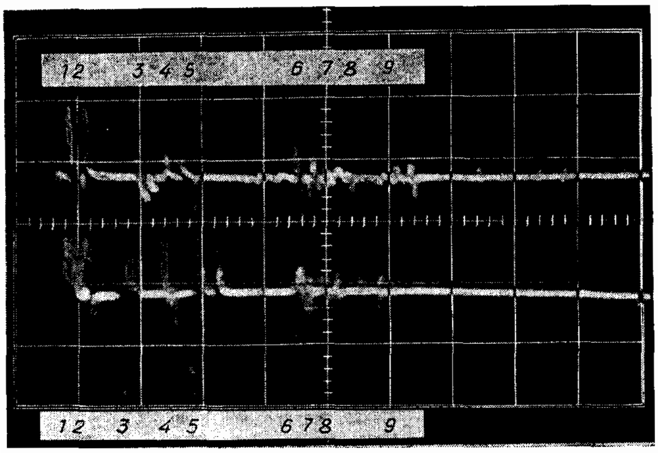

FIG. 8. Records of the high-frequency component of seismic signals at separated sensors. The timebase is 0.5 ms/division. The plate is 40 cm long. The numbers enumerate the bursts that were compared.

ten such bursts are obtained during the fracture time. This time corresponds to a penetration velocity $v_\perp = d/T \approx 3 \cdot 10^2$ cm/s. The value of this velocity is surprising. It is three orders of magnitude lower than the velocity of seismic waves that is used to estimate the duration of an earthquake.[5] It disagrees not only with the preconceptions but also with specific estimates (10^5 cm/s) obtained from seismograms.[8,13,16]

It was not difficult to analyze this discrepancy, since in the model experiment many bursts were emitted as the rupture was formed. They have distinct starting points and can be identified as separate signals, i.e., the records of these bursts made with separated sensors can be compared[14] (see Fig. 8, which shows records of seismic signals which were made with separated sensors and were filtered so as to suppress frequencies lower than 10 kHz. The arrangement of the sensors is shown in Fig. 6. The delay time τ_i of the compared signals (20–100 μs) is explained by the difference of the signal propagation times. The measured value of the delay can be employed to determine the position of the source:

$$c_s\tau_i = [h^2 + (l + x_i)^2]^{1/2} - [h^2 + (l - x_i)^2]^{1/2};$$

here x_i is the displacement of the source relative to the center of the plate, h is the distance from the sensors to the location of the rupture (1 cm in the experiment), l is one-half the width of the plate, and $c_s \approx 3.4$ km/s is the estimated propagation velocity of the waves. The results of the interpretation are shown in Fig. 9. One can see that most sources are located on the boundaries of the plate ($x_i = l$). This result confirms the intuitive rule for regarding the rupture surface in an earthquake as the region of the aftershock process. It also agrees with the experimentally established fact[16] that the region of the aftershock process is divided into two subregions separated by the rupture boundary. If the rate of the process is estimated as the rate of displacement of the sources of successive bursts, then the model experiment gives the estimate $v_\parallel \approx 3 \cdot 10^4 – 2 \cdot 10^5$ cm/s. This agrees well with the estimates obtained by seismologists.

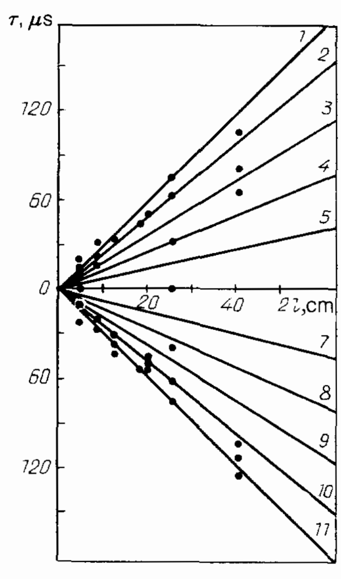

FIG. 9. The interval between the compared bursts as a function of the width of the plate. The lines *1–11* correspond to radiation from the boundaries of the sample and the lines *2–10* correspond to radiation from a distance 2*l* from the boundary.

Thus the process of rupture formation is strongly anisotropic. It propagates with a high (seismic) velocity along the groove and with a low velocity of the order of 1 meter per second into the sample (while repeatedly oscillating along the groove). Filming confirms that in those cases when the sample appeared in a frame at the moment when the rupture had already started but was not yet completed only a single process occurs between aftershocks. In the photograph of Ref. 14 it is clearly seen that the rupture penetrates into the glass over the entire front and along the entire groove.

The formation of a rectilinear wavefront slowly penetrating into the body of the object undergoing fracture can be easily modeled by the unsticking of a roll of sticky tape (scotch tape). When the end of the tape is pulled, the rupture at first straightens out rapidly and becomes parallel to the axis of the roll. Then the tape slowly tears away from the roll along the entire front at once, as a result of which the surface of the piece of tape that tears away from the roll remains lineal. The phenomenon moves with a velocity of 1 cm/s, and its characteristic features can be observed without the use of any special instruments. It can be seen that a rupture forms each time at the edge, straightens out the front up to the other edge, is formed again, etc.; in the process one can see under a microscope tracks in the form of parallel straight lines on the freshly formed surface. The seismic signal formed when the tape is unrolled also consists of a series of bursts; this series is shown in Fig. 10.

Thus the materials used for observing the breaking of glass reveal an interesting feature of the breaking process: The rate of growth of the rupture surface is anisotropic. This growth rate is equal to the seismic velocities for motion parallel to a preformed crack and is comparatively low in the transverse direction. This feature reveals a new and interesting property of the rupture process: the penetration velocity $v_\perp$ of the crack. The value of this velocity significantly affects the macroscopic effects of fracture. The mechanical momentum transferred to fragments as a result of the opening up of the rupture is proportional to the duration of the process ΔT and is therefore inversely proportional to the velocity. It can be estimated as

$$p_i \approx \sigma_{ik} S_k \Delta T \approx \sigma_{ik} S_k \frac{d}{v_\perp}$$

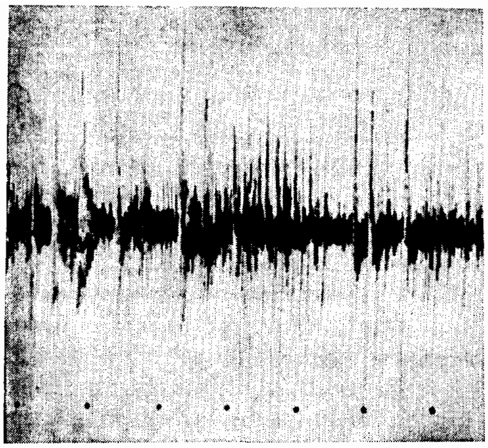

FIG. 10. The seismic signal generated during the formation of the rupture surface when scotch tape is pulled from a roll. The time interval between the markers is 1 s.

(σ_{ik} is the stress which is removed by the rupture and S_k is the area of the rupture), i.e., some of the energy released in the motion of the fragments is inversely proportional to the squared velocity of penetration of the crack. For low velocities it can become large. In particular, in the experiments with glass it was equal to about 10% of the stress energy; this was determined from the period of oscillations of the fragment lying on the surface of the table. The latter fact may turn out to be important for interpreting earthquakes. We shall summarize the main conclusions which are important for the interpretation of seismic signals from earthquakes.

1. The main shock is not the process of rupture formation, but rather it is the signal indicating the start of this process.

2. The evolution of the rupture process can be determined by interpreting the aftershocks—the maxima of the intensity which are delayed relative to the main shock and are emitted from the rupture surface at the moment when the process encounters nonuniformities or its direction of propagation changes. The rupture process is observed as emission from a moving source.

3. AN EARTHQUAKE AS A MOVING SOURCE OF SEISMIC RADIATION

The simplest representation of an earthquake as an instantaneous point source does not describe the local features of the phenomenon and the characteristics of its evolution in time. It can be augmented with observations of the characteristics of seismic radiation. The sources of this radiation are distributed very nonuniformly in space and time. Its maxima can be regarded as a sequence of separate instantaneous sources lying along the trajectory of the process. Assuming that the process propagates continuously between these points, we obtain a representation of the process as a moving radiating point. The trajectory is determined by the world points of successive maxima.

Such a representation contains quite detailed information about the spatiotemporal evolution of the earthquake, and it can be used as a basis for studying the pattern of development of different phenomena accompanying an earthquake (tsunami generation, horizontal motions, seaquakes).

We shall mention some properties of the trajectory. We shall use the observational data for the Alaskan earthquake of March 28, 1964.[17] Successive radiation maxima and their coordinates and times in the source are presented in Table II. The development of the process is illustrated in Figs. 11a–d. Figs. 11a and b show a track of the trajectory on the earth's

TABLE II. Parameters of aftershocks.

Aftershocks						Aftershocks					
in Ref. 7	No.	Time at the source, h/min/s	Coordinates		Magnitude, M	in Ref. 7	No.	Time at the source, h/min/s	Coordinates		Magnitude, M
			λ, °N	φ, °W					λ, °N	φ, °W	
5	1	3.36.14	61,05	147,48			29	6.15	60	149	
	2	3.38.50	59,7	147,2	8,1	19	30	6.24.13	59	148,3	4,7
	3	3.41.15	59,2	148,5		20	31	6.29.15	57,7	151,3	4,9
	4	3.44	59	150		21	32	6.32.40	60,9	147,6	5,5
	5	3.48.20	58,2	151		22	33	6.36.50	57,4	152,5	5,2
	6	3.52.10	57,5	153,7		23	34	6.41.28	59,0	147,8	5,5
	7	3.56.20	59,0	148,1		24	35	6.42.57	57,98	151,6	5,2
	8	4.02.40	58,7	148,3		25	36	6.43.54	58,2	151,2	6,1
	9	4.05.45	56,5	153,8		26	37	6.50.48	56,9	151,7	5,1
	10	4.10.25	59,0	146		27	38	6.53.35	58,8	149,5	5,7
	11	4.14.0	56,0	154		28	39	6.59.50	56,3	153,3	4,8
	12	4.24.0	57	153,5		29	40	7.02.30	58,6	150,8	4,8
	13	4.28.15	59,5	149		30	41	7.03.58	56,6	152,9	4,8
	14	4.38.0	57,5	152		31	42	7.09.07	59,8	148,1	5,3
	15	4.42.0	58,5	150		32	43	7.10.22	58,8	149,3	6,0
8	16	4.54.10	59,8	149,3	6,1	33	44	7.16.16	58,0	150,7	5,3
	17	5.06	59,5	149		34	45	7.24.25	59,6	148,7	5,1
9	18	5.17.21	60,4	146,7	5,1	35	46	7.28.18	57,5	151,3	5,0
10	19	5.31.20	57,4	151	5,2	36	47	7.30.29	57,3	151,7	5,6
11	20	5.33.50	60,05	146,4	5,5	37	48	7.39.15	59,1	149,1	4,6
12	21	5.35.40	57,2	153	5,8	38	49	7.44.08	59,5	146,5	5,0
13	22	5.38.19	60,8	147		39	50	7.47.44	58,14	150,5	4,9
14	23	5.42.40	64,7	150,2	5,3	40	51	7.48.48	56,9	153,3	5,1
15	24	5.44.5	60,1	148,8	4,9	41	52	7.50.22	56,4	152,7	5,0
16	25	5.46.30	59,0	149,1	5,4	42	53	7.52.08	56,4	152,8	4,7
17	26	5.49.30	56,3	154	5,1	43	54	7.55.06	58,2	150,4	4,5
	27	5.55.30	60	145		44	55	7.59.40	57,9	151	4,7
18	28	6.08.45	60,15	148,5	5,5	45	56	8.05.23	59,9	150,1	4,7

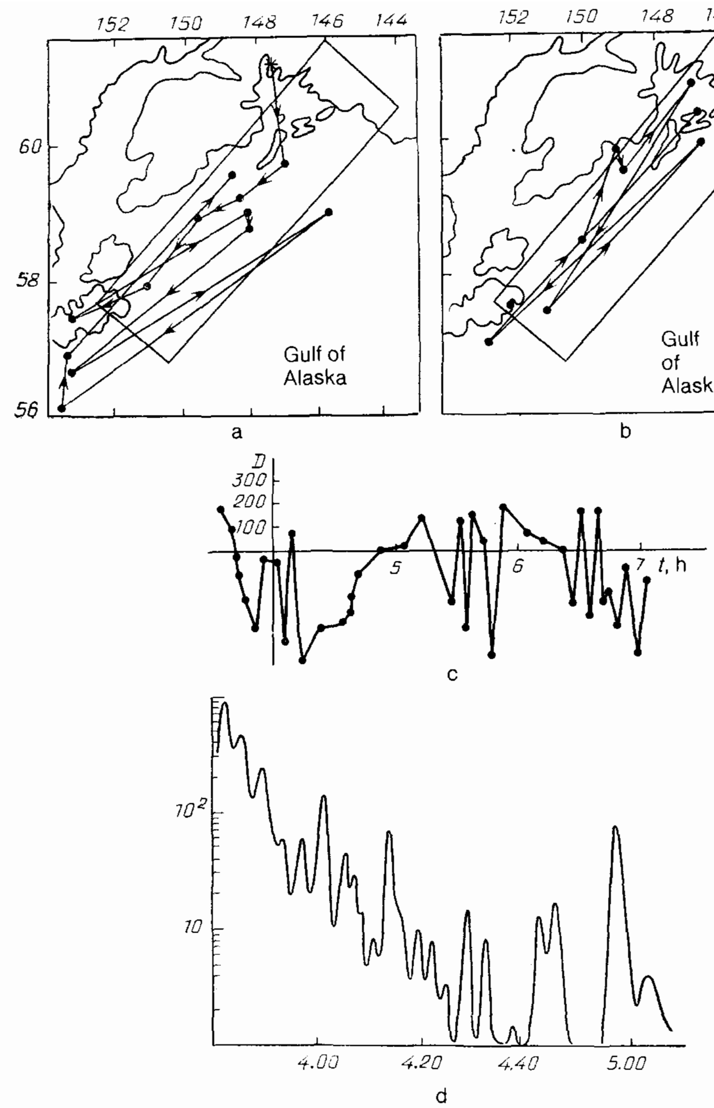

FIG. 11. The trajectory of the source of seismic radiation for the March 28, 1964 earthquake in Alaska. a) The track of the first stage of the trajectory. b) The track of the second stage of the trajectory. c) The time dependence of the displacement of the source. d) The time dependence of the intensity of the radiation.

surface. Figure 11c shows the temporal unfolding of the projection of the trajectory on the long axis of the dislocation plane; the temporal unfolding was determined in Ref. 18 from the results of the interpretation of the deformations of the earth's surface. Figure 11d shows the time dependence of the radiation intensity during the first hour of the evolution of the process.

One can see (see Fig. 11a) that the radiating point moves in the plane of residual dislocations. The radiation maxima lie, as a rule, at the turning points of the trajectory, which roughly coincide with the boundary of the dislocation plane. This completely confirms the results of the analysis of seismic signals generated by the breaking of the glass plate. The points 1-6, 14–18, and 27–30 of the trajectory are exceptions. On these sections the process evolves approximately in the direction of the principal axis of the dislocation plane and it is accompanied by a large number of intermediate maxima, which are not observed as the glass plate is broken.

Analogous features are also observed on a map of the temporal evolution of the source (see Fig. 11c). The section of the trajectory shown in the figure separates into three stages. The first stage (points 1–13) contains two phases. During the first phase the source moves slowly in the direction of the principal axis of the dislocation plane and during the second phase it oscillates along this axis within this plane. The characteristics of the second phase simply agree with the data obtained from the model investigation. The source moves between the boundaries with a velocity of 1.4–2.6 km/s. The process propagates along the groove with seismic velocities. The section of trajectory from the point 14 to the point 18 does not have an analog in the model experiment. On this section the process propagates relatively slowly (0.5–1.0 km/s), a large number of intermediate bursts are emitted, and the direction of motion of the overall process remains unchanged. In Ref. 13 this phase is called the leader stage by analogy to the process of a lightning discharge,[19] which, as is well known, is preceded by a leader which forms the propagation channel of the discharge.

The leader phase and the rupture phase apparently comprise the first stage of the earthquake. The second stage (points 14–25) also starts from the leader phase (points 14–18), which after the point 18 transforms into oscillations. These oscillations (see Fig. 11b) occur in a somewhat different plane. The position of the northeast boundary of the plane changes, and the principal axis along which the oscillations occur is tilted by 5°. After the second stage is completed, the third stage starts with some delay, etc. A total of six stages, whose total duration is about 12 h, can be clearly distinguished in the process. Separate bursts of radiation are also observed with long delays (days and longer), but they do not form a complete stage, and the leader phase is not terminated by an oscillatory process.

Thus the earthquake process can be represented by a sequence of several completed stages, each of which contains two phases: a leader phase, when, from our viewpoint, a groove is formed along which damage later occurs, and an oscillatory phase, which, following the data of the model experiment, can be regarded as the formation of a rupture plane. The duration of a separate stage depends on the size of the focus and is equal to several tens of minutes. There can be several stages; the foci of each stage differ somewhat.

We shall discuss the characteristics of the variation of the radiation intensity (see Fig. 11d). The overall features are identical to those of the radiation emitted when the glass plate is broken: The radiation consists of separate bursts, and the highest bursts start and terminate the rupture formation process. However some differences are observed. First, during the leader phase the signal is emitted practically continuously. Instead of separate bursts, continuous emission is observed and the emission maxima are two to three times stronger than the background. The second difference is that although the amplitudes of the maxima starting and terminating the formation of the rupture are actually higher than the amplitudes of the intermediate maxima, they are nonetheless significantly lower than the main maximum that is emitted during the leader phase of the process and determines the magnitude of the earthquake.

Thus the characteristic features of the change in intensity of the radiation from a point source are correlated with the motion of the source. At the leader phase the radiation consists of a large number of bursts, the strongest of which do not always start the process (at the first stage, this is the second maximum). The radiation maxima at the second phase of the stage, as a rule, arise at the ends of the trajectory, where the direction of motion is reversed. The second, third, etc., stages are characterized by the same features, and this is what makes this representation of the process physically meaningful.

4. RELATION BETWEEN THE PARAMETERS OF THE TRAJECTORY AND TSUNAMIS

The representation of an earthquake by a moving point from which seismic waves are emitted can be used to analyze the spatiotemporal evolution of the aftereffects. On the basis of the number of disasters caused, the most interesting aftereffects are tsunamis and deformation of the earth's surface. In what follows the characteristics of tsunami generation are analyzed for the example of the March 28, 1964 earthquake in Alaska.

In engineering calculations tsunami generation is ususally described by the piston mechanism. In this method it is assumed that a tsunami is generated as a result of an instantaneous rise of the sea bottom occurring uniformly[20] or nonuniformly[21] in space in the focal area of an earthquake. This is the simplest model. It describes the phenomenon qualitatively, but it practically does not reflect at all the characteristics of the temporal evolution and the spatial distribution of the wave. These characteristics are very varied, and it is helpful to take them into account when making a forecast. In particular, this model does not describe the 8-h delay of the tsunami in Seldovia and the 6-h delay in Cordova for the earthquake of March 28, 1964. These points lie within the focal region, and the theoretical delay is equal to zero. Thus the problem of tsunami generation during an earthquake cannot be regarded as having been solved, as is sometimes done in the official and scientific pronouncements.

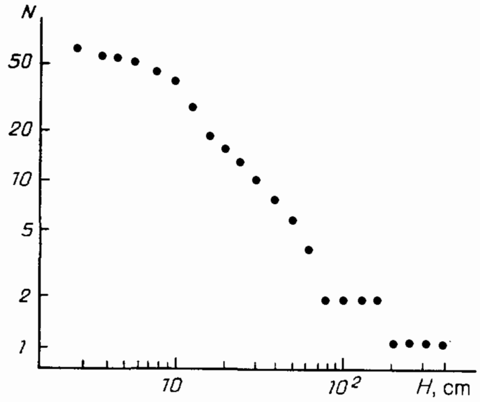

FIG. 12. The number of tsunamis recorded in Miyako (Japan) as a function of the wave amplitude.

We shall examine below two questions regarding this problem: Which characteristics of the trajectory determine the position of the focus of the tsunami, which in turn determines the time of arrival of the tsunami at different points along the coast? Which characteristics of the trajectory are related with the generation of intense waves and determine their direction of propagation and the region of space where they appear?

A tsunami is a complicated concept. Tsunami-related long-period waves on the sea surface always arise during earthquakes and, as a rule, their amplitudes do not exceed 20–30 cm. [Figure 12 shows the distribution of the frequencies with which tsunami waves with different amplitudes appeared in Miyako (Japan).] Such waves do not exceed the high tide and are of interest for science as a source of information about earthquakes. There is no need to sound a general alarm for such waves; such alarms only discredit warnings. But very rarely and, as a rule, along short sections of the coastline (from 10 to 100 km long) there arise waves whose height exceeds 5 m. These are destructive waves: They wash away vegetation,[2,22] they demolish buildings, and people caught in such a wave rarely survive. For this reason, of the questions listed above the second one is the central question for organizing a reasonable tsunami warning system.

The region of the ocean surface bounded by the tsunami wavefront at the moment T_0 of the main shock of the earthquake is usually called the *tsunami focus*. The question is how to estimate this boundary from the seismic signal.

The answer depends on two assumptions: The first assumption is that the tsunami and the seismic oscillations are two different types of radiation generated by the same process from the same source and the second assumption is that a tsunami is generated when the source lies beneath the ocean or sea surface.

A moving point source of seismic radiation does not lead to a point source of the tsunami, because the source moves and its velocity is greater than that of the tsunami. The contour of the source, defined as the envelope of inverse isochrones,[20] in this case is not a physically meaningful concept—the wavefront; it is the analytic continuation of the wavefront formed by some time T_2 up to the moment of the main shock T_0 ($T_0 < T_2$). On the basis of these remarks one can see from analysis of the trajectory of the seismic signal of the Alaskan earthquake (see Table II) that the wavefront started to form at the time $T_1 = 3$ h 39 min, when the trajectory emerged from Montague Strait, i.e., it was delayed by 3 min relative to the main shock. It continued up to the time 3 h 52 min (the point 6 of the trajectory), when the direction of motion was reversed. The wavefront formed by the time $T_2 = 3$ h 52 min can be constructed as an envelope to the wavefronts excited from all identified intermediate points of the leader phase of the trajectory. These are the points *2–6*. In so doing, a circle with radius $c(x_i,y_i)\cdot(T_2 - T^i)$ is drawn from each point x_i, y_i, T^i; $c(x_i,y_i)$ is the velocity of the tsunami at the point x_i, y_i. The envelope of these circles is the wavefront sought. The curve is shown in Fig. 13 and is virtually identical to the results of the reconstruction of the wavefront which were refined in Ref. 23. We note a feature of the wavefront. It is a wave from a rapidly moving source, known in hydrodynamics[24] as a ship wave on shallow water. It is sharply directed—the radiation maxima are concentrated around the angles $\theta = \pm \arccos(c/v_\parallel)$ from the direction of motion.

To reconstruct the tsunami focus the wavefront must be analytically continued up to the moment of the main shock

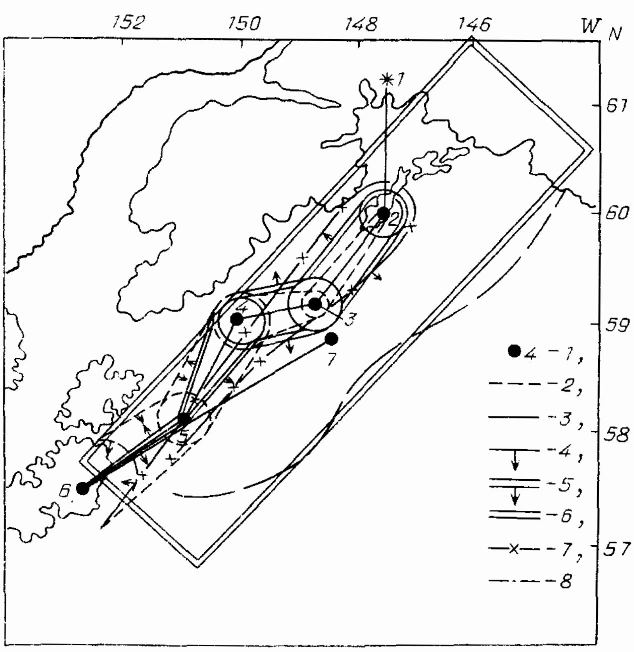

FIG. 13. Reconstruction of the tsunami focus from the trajectory of the seismic signal. *1*) The positions of successive maxima of the seismic radiation, *2*) isochrones corresponding to the times $T_6 - T_i$ (negative radius of curvature), *3*) isochrones corresponding to the times $T_6 - T_i$ (positive radius of curvature), *4*) tsunami focus along the trajectory, *5*) tsunami wavefront at the moment of formation, *6*) projection of the dislocation plane, *7*) tsunami focus reconstructed by Pararas and Caroyannis, *8*) tsunami focus reconstructed by van Dorn.

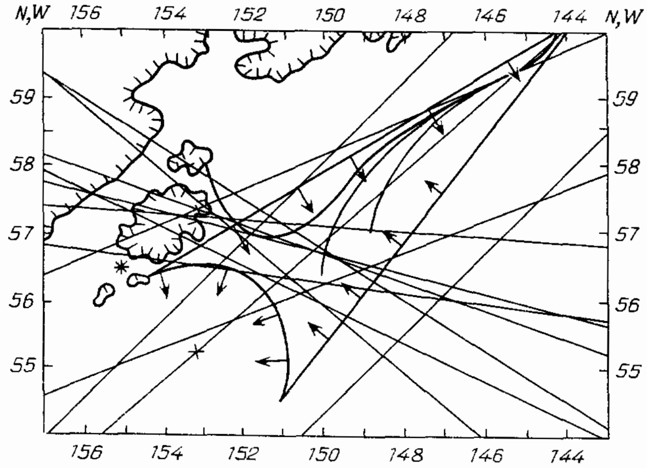

FIG. 14. Average focus and inverse isochrones from results of distant observations.

T_0. In the case of the Alaskan earthquake this shock was subterranean and a tsunami was not generated. For this reason, it is not the actual front that appears in the role of a focus, but rather its analytic continuation up to this moment in time. The analytic continuation of the wavefront from a point source up to a moment in time when the wave still did not exist is a circle with a negative radius of curvature, equal to $-c(T_2 - T_0)$. For this reason, the analytic continuation of the wavefront containing two instantaneous point sources contains concave sections with a negative radius of curvature; these sections are shown in Fig. 13 in the neighborhood of the points of onset of generation and change in the direction of motion of the seismic source.

The latter circumstance was overlooked in works on the reconstruction of earthquake foci.[20,25] The reason is that the problem of constructing the envelope of the inverse isochrones is improperly posed. As a result, the family of isochrones does not have an envelope at all; this is shown in Fig. 14, where the inverse isochrones for the tsunami of March 28, 1964 are shown.[26] Usually some arbitrariness is allowed and the inner envelope is constructed. Such a focus does not give a correct estimate of wave direction. To obtain a correct estimate the model of the contour must be parametrized. The simplest model is a focus of a uniformly moving point. In this case the focus consists of two arcs of circles centered at the points *1* and *2* (the start and end of the motion) with radii $-c_2(T_2 - T_0)$ and $-c_1(T_1 - T_0)$. To complete the contour these arcs must be connected by common tangents. Such a focus, constructed from the arrival times of the tsunami at points on the coastline of the Pacific Ocean,[27] was constructed in Ref. 26 for the March 28, 1964 tsunami[28] and is shown in Fig. 14. It differs appreciably from the point-like focus constructed from near-zone data, but it contains a section with a negative radius of curvature, which corresponds to a delay of wave generation $T_2 - T_0 \approx 15$ min; this is in complete agreement with estimates based on the seismic trajectory.

Comparing the results presented shows that the trajectory of the seismic signal provides quite accurate information for constructing a tsunami focus. This estimate is of better quality than the estimate based on the far-zone inverse isochrones, and its quality approaches that of the estimate based on records of the arrival time of the wave at points close to the source.

We note that in order to form an idea of the focus of a tsunami two points of the trajectory are significant: the point at which the trajectory first emerges to beneath the ocean surface and the point at which the velocity of the seismic source is equal to or drops below the velocity of the tsunami wave.

The reconstruction of a tsunami focus is used to solve two problems: the estimation of the arrival time of the wave at different coastal points and the estimation of the propagation direction of the wave—the section of the coast where the largest waves should be observed. An estimate of the focus based on the seismic source gives the correct answer to the first question and an inaccurate answer to the second question. The point is that the tsunami wavefront is not the main damaging factor. In some cases the wave starts with ebbing of the water while in other cases it starts with a slow rising of the water level (Fig. 15). The steep waves that degenerate into a bore on the shallows are the damaging waves. In the record shown in Fig. 15 of the March 28, 1964 tsunami in Sitka this is an intense peak delayed by 25 min relative to the front. Its amplitude is several times greater than the rise in water level on the wavefront. Judging from the delay this peak was generated not during the leader phase, but rather during the oscillations occurring in the process of formation of the rupture plane. This is not accidental. At the second and third stages of development of the process the maximum waves were also observed only after the leader phase is completed. The distinguishing feature of this stage of the process are the high velocities of the source; this is apparently more important than large amplitudes of seismic radiation at the leader phase. The latter was pointed out in Ref. 29, where a strong correlation was observed between the high-frequency peaks of a tsunami and the phases of unipolar motion of the source of the seismic signal. We note that the damaging high-frequency wave is sharply directed as a wave from a source propagating with velocity higher than the velocity of the radiation. The direction of emission is different from the normal to the source and makes an angle $\theta = \arcsin(c/v_{\parallel})$. In this case, at the first stage the wave was found to be directed toward the section of the coast between Yakutat and Tasu Sound, where an alarm should have been sounded. Since the source oscillates, there are two such directions: one corresponds to the west-to-east phase of the motion and the other corresponds to the east-to-west phase. The latter phase turned out to be destructive for the Hawaiian Islands. The generation times of these waves are different, so that in analyzing the high-frequency component of the radiation certain difficulties arise in connection with the incompatibility of the sources for different directions of propagation.[29]

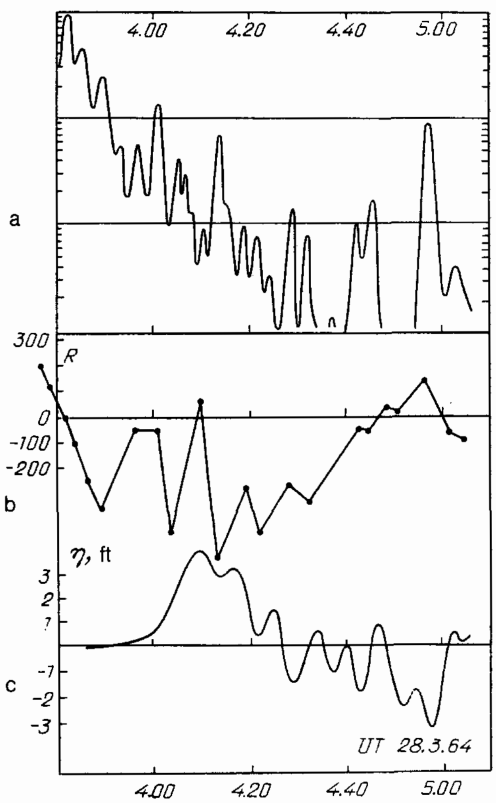

FIG. 15. Comparison of the temporal variations of the amplitude of the seismic signal (a), the distance traversed by the source (b), and the tsunami waves (c).

At each stage of development of an earthquake the direction of the axis of oscillations and the direction of excitation of the intense wave change. The waves generated at the second and third stages were directed toward other points along the coast. In particular, the maximum wave at Crescent City was associated with the third stage.

One can see that by analyzing the trajectory of a seismic source it is possible to determine reasonably well the region where an alarm should be sounded: only at locations toward which the destructive wave is directed and only for a time that can be calculated if the generation time is known.

5. RELATION BETWEEN THE ELEMENTS OF THE TRAJECTORY AND DEFORMATIONS OF THE EARTH'S SURFACE

The objective characteristics of earthquake damage are the deformations of the earth's surface. In the instantaneous-point-source model the deformations are described on the basis of the seismic moment tensor M_{ik}, which is assumed to be proportional to the symmetrized sum of two dyads S_i and b_k, where S_i is the area of the rupture surface and b_k is the dislocation on the rupture. The directions of the vectors and the products of their lengths are estimated from the seismograms. The quantities $|S|$ and $|b|$ are specified using the averages given in Table I. Using the data on the epicenter of an earthquake and the depth of the focus and the values of S_i and b_k, the static problem of the theory of elasticity in a half-space with a known dislocation on a given plane is solved by calculating the horizontal and vertical displacements of the earth's surface.[30,31] It is assumed that the deformation is established after the passage of the surface or transverse wave, if the latter waves are still not distinguishable.

This is not a very accurate representation. Estimates of the vectors S_i and b_k are usually corrected after the tsunami is recorded and after a geodesic survey of the location is made.[18] For the March 28, 1964 earthquake, two planes S_i^1 and S_i^2 having the same orientation but different size were introduced in order to achieve consistency with the results of the geodesic survey. The larger area corresponded to a small dislocation vector and the smaller area corresponded to a large vector. The large area described the asymptotic deformations at large distances and the smaller area described the asymptotic deformations in the focal zone. Even such deeply *a posteriori* representations must be further refined. They describe only the average picture and do not touch upon the details, in particular, the gradients of the deformations. These details are very significant, since they determine the pattern of the damage that actually occurs. Returning to Fig. 4, we call attention to the fact that the average *a posteriori* picture describes the region of damage much more accurately: Montague Island, the cities of Whittier, Seward, and Valdez lie on the projection of the dislocation plane. However, even this *a posteriori* estimate is not completely accurate. In particular, the damage in the towns of Portage and Turnagain Heights (Anchorage) occurred far from this plane, so that it is still important to refine the description of the dislocations.

It is difficult to expect that the solution of the problem will be an average, statistically well-founded representation of an earthquake. The problem is that the locations of strong damage are oddly scattered over the region of the focus. In Ref. 2 it is pointed out that at some locations, more than 100 km from the source, it is impossible to indicate the magnitude of the vibrations. It changes from 10 in one part of the city to 7 in another.

The estimate of the evolution of the damage (development of damage in time) based on the idea of a rapidly evolving rupture is also apparently unsound. The results of the model experiment show that the deformations arise not in the process of rupture formation and not at the moment at which the first signal is emitted, but rather only after the rupture has formed and the fragments begin to move relative to one another.

Transferring to the representation of an earthquake by a moving radiating point source expands the possibilities of interpreting the signal for estimation of deformations. From the model experiment it follows that the track of the trajectory covers the rupture surface quite densely and contains information about the position and the formation time of the rupture. In the following analysis we shall confine our attention to the solution of the following questions:

1. Which features of the deformations accompanying an earthquake are related with opened fractures?

2. How should the position and time of an opened fracture be determined by analyzing the trajectory of the seismic source?

First question. We shall examine the deformations occurring during the March 28, 1964 earthquake.[32-34] They are divided into vertical u_z and horizontal $\mathbf{u}_p$ displacements.[32] The vertical displacements are shown in Fig. 16. The map can be divided into two distinct regions: an interior region, concentrated in the region of the focus, where the deformations are positive (the surface rises), and the exterior region, where the displacements are negative. The interior region is a ridge up to 30 feet high with a virtually rectilinear axis. The ridge is 100 km long, but its exact length was not determined because not enough measurements were made. The main shock occurred on the northeast boundary of the ridge. The region of positive displacements was about 20 km wide.

Negative displacements are observed in a wider region.

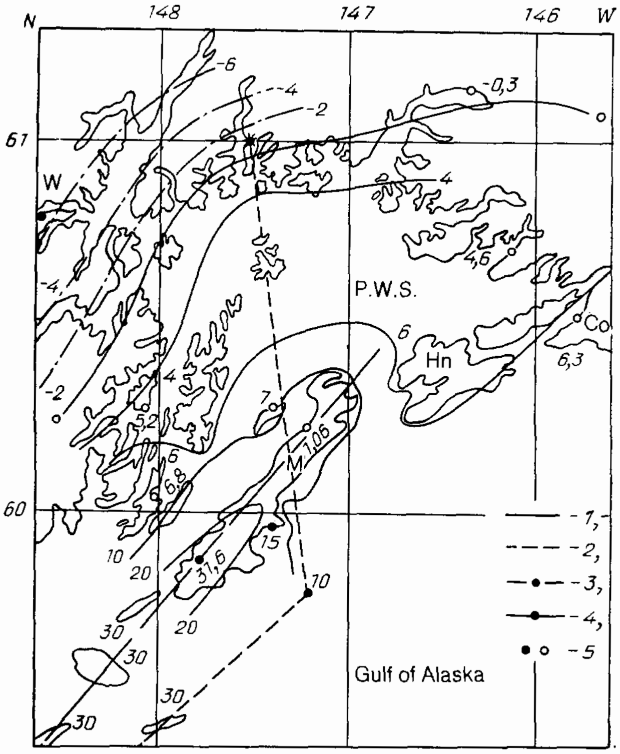

FIG. 16. Vertical displacements in the northeastern part of the focus of the March 28, 1964 Alaskan earthquake. *1*) Isoline of positive displacement, *2*) isoline of negative displacement, *3*) axis of the ridge arising with the earthquake, *4*) track of the leader phase of the first stage, *5*) points of the measured variations of the residual level from tidal oscillations. W—Whittier, b. R—Resurrection Bay, Co—Cordova, M—Montague Island, H—Hinchinbrook Island.

The epicenter of the earthquake lies on the boundary of the regions of positive and negative displacements. Jumps of the displacements on faults are observed in a detailed underwater survey near the island of Montague, but they were not followed over large distances.

The information on horizontal displacements was analyzed in greater detail.[33] The horizontal displacements are characterized by magnitude and direction. They are two-dimensional vectors. The horizontal displacements constructed based on the measurements are shown in Fig. 17. The following features are observed.

1. The lines tangent to the deformation vectors (rays) emanate from a single point (63° N, 150° W), which is not the epicenter and, moreover, does not even lie in the region of the focus. It lies in the McKinley massif. The displacement at the point itself is equal to zero.

2. The rays are practically rectilinear and they are directed toward the focus of the earthquake. The largest directional variations are visible only at the boundaries of geomorphological formations.

3. The magnitude of the displacement vector, equal to zero at the point of emergence, increases monotonically toward the focus, near which it has a maximum of 50–70 feet. The dependence of the deformations on the distance to the axis of the dislocation plane is shown in Fig. 18. The only characteristic point of this dependence, aside from the maximum, is a point of inflection. It lies approximately on the boundary of the region of positive and negative displacements.

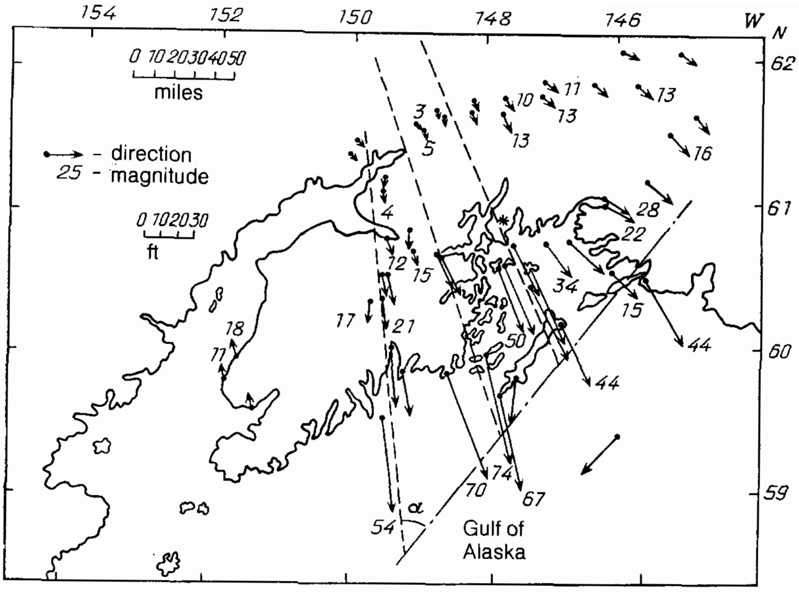

FIG. 17. Map of the reconstruction of the horizontal displacements of the earth's surface during the March 28, 1964 Alaskan earthquake.

The horizontal displacements are directed toward the rupture plane but they approach its axis at different angles α, which are apparently largely determined by the geomorphological features of the region.

A more detailed relation between the geomorphological features and the directions of the horizontal displacements is obtained from analysis of the tensor of deformations. Figure 19 shows the values of the tensor of deformations, which were calculated from the horizontal displacements.[34] Two mutually perpendicular segments are shown; their lengths are proportional to the principal values of the tensor and they are oriented along the principal unit vectors.

The position of the rupture plane is determined by the location where the difference between the principal values is maximum; the boundary between the mobile fragments is also the bisector of the angle between the unit vectors. The bisector is chosen on the basis of information about rotation. This information is presented in Ref. 34, and it reduces to the fact that above the axis of the earthquake the rotation is clockwise while below it the rotation is counterclockwise. The corresponding lines are presented in Fig. 19.

The dashed lines in Fig. 19 indicate the faults which move during an earthquake. They are also the geomorphological faults and can be determined beforehand from a geographical map. In particular, the line *aa* is a fault that passes through Resurrection Bay, Kenai Lake, and Quarry Canyon; the line *bb* is a fault that passes through Wells Inlet, Portage Lake, and Turnagain Arm.

The rays of the horizontal displacements lie practically along the directions of the faults along which the movements occurred.

Thus the faults play an important role in the formation of the pattern of horizontal displacements, a significant fraction of which is determined by the relative motion of fragments along the faults.

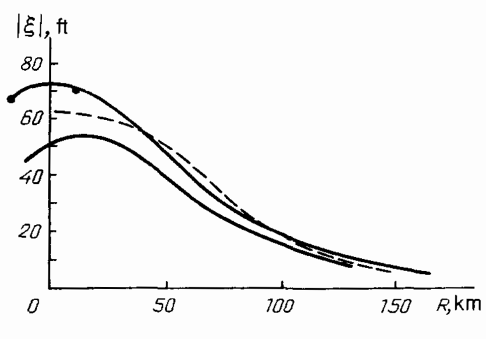

FIG. 18. The dependence of the amplitude of horizontal displacement on the distance from the axis of the focus.

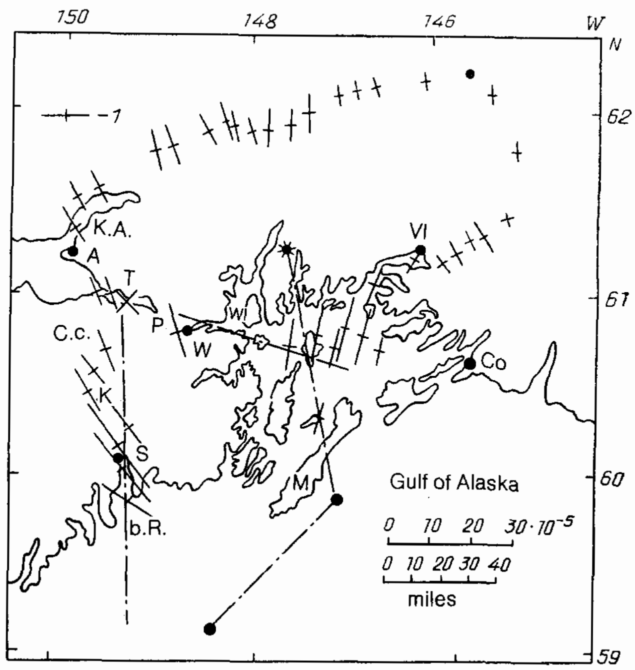

FIG. 19. Results of calculations of the tensor of deformations. A—Anchorage, W—Whittier, Vl—Valdez, C.c.—Creek Canyon, K—Kenai Lake, K. A.—Knock Arm, Co—Cordova, M—Montague Island, P—Portage Lake, S—Seward, T—Turnagain Arm, Wl—Wells Inlet. *1*) Principal axes of the tensor of deformations in the scale shown in the legend.

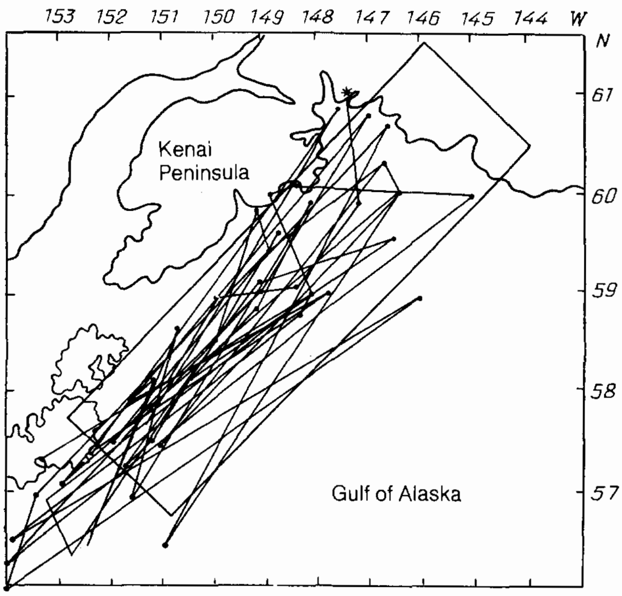

FIG. 20. Track of the trajectory on the earth's surface.

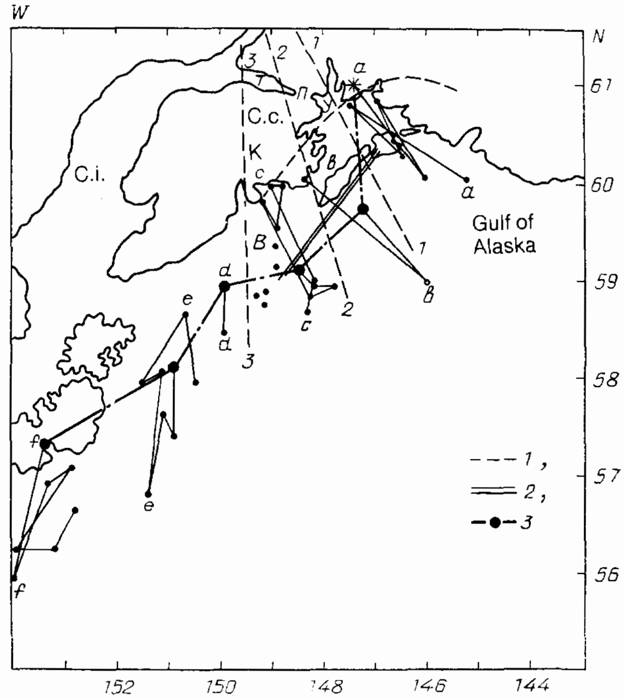

FIG. 21. Mobile faults and characteristics of the track of the trajectory. *aa, bb, cc, dd, ee, ff*—transverse faults constructed from analysis of the trajectory. C.i.—Cook Inlet, C.c.—Creek Canyon. *11, 22, 33*—Rays of horizontal displacements, used for analyzing the spatial dependence of the horizontal displacements. *1*) Boundary of the region of positive and negative displacements, *2*) ridgeline of positive vertical displacements, *3*) leader crack and position of maxima.

Summarizing the observations, we shall single out the characteristic elements that should be determined along the trajectory of the seismic source. These are the axis of the ridge of vertical positive displacements and the position and direction of the faults along which movement has occurred.

The *track of the trajectory* on the surface is shown in Fig. 20. The broken line covers quite densely the focal region of the earthquake, i.e., it makes it possible to describe, in complete agreement with the model experiment, the average pattern of deformations in space, without revealing the faults along which the motion started. However, the blackened region contains many maxima of seismic radiation which were not interpreted. Analysis of the separate phases of the trajectory shows that at a certain stage of the process it is precisely the interior points that served as the boundaries along which the process evolved. By regarding each stage as the formation of a separate rupture plane it is possible to reconstruct the interior boundary. The results are shown in Fig. 21. The curve of the boundaries of separate fragments consists of the broken line *abcdef* and contains six transverse segments *aa*,..., *ff*. Each segment is correlated with a geomorphological fault. The segment *aa* coincides with the fault passing through Turnagain Arm, Portage Lake, and Wells Inlet; the segment *cc* coincides with the fault passing through Resurrection Bay, Kenai Lake, and Quarry Canyon; and the segment *ff* corresponds to Cook Inlet. Some of these segments coincide with mobile faults identified in the analysis of the horizontal deformations; the rest fall outside the region of the measurements, i.e., the boundaries of the faults which opened for the relative motion are determined by the elements of the track of the trajectory.

We note that all these faults can be discovered from the track of the leader phase of the first stage, which contains radiation maxima that lie on the intersection of the axis of the earthquake and the plane of the opened fault.

Thus observations of the trajectory (even observations of only the leader phase of the first stage) permit determining the position of the transverse mobile faults, if the geomorphological features of the region are known.

We note that since many faults start to move simultaneously and the signals from different boundaries are emitted at random times, in order to reconstruct the contour of the mobile fault the coordinates of the successive maxima of radiation from some neigborhood of the maximum lying on the track of the leader of the first stage must be connected.

The character of the evolution of the trajectory shows that faults do not open up simultaneously. The delays are equal to minutes and tens of minutes for the first phase and hours for the second and subsequent phases. This is the lead time available for early warnings of these phenomena, which lead to disasters that occur not only as a result of maximum accelerations in the seismic wave but also as a consequence of the motion of fragments of the earth's crust along the faults. The latter motions are confined to the location through which the fault passes and occur at a time when this fault started to move.

This conclusion is supported by assessments of the earthquake damage shown in the map of Fig. 4. The regions of damage are concentrated near faults and the points of the maximum (magnitude 9, 10, and 11) vibrations are concentrated at the triple points where two faults intersect.

Clear evidence of the localized nature of the damage was found for the July 10, 1958 earthquake in Alaska. The leader crack passed along the Fairweather fault, on which it left a ~ 10 m wide track of levelled trees; this track widened up to several kilometers as it approached lakes. Immense damage occurred at articulations with a transverse geological formation—Lituya Bay. In addition, phenomena such as standing waves on the earth, geysers of sand and water, and the appearance of cracks were delayed relative to the moment of passage of the seismic wave by several tens of minutes.

6. METHOD FOR ESTIMATING THE TRAJECTORY OF AN EARTHQUAKE

At both large and insignificant distances from the source, a seismic signal is a sign-alternating series of bursts with characteristic periods ranging from 0.1 to 200 s and a total duration of several days (see Fig. 1). Separate intense bursts, hundreds of times stronger than the background radiation, can be clearly identified in this series at times exceeding 1 hour from the front. On each of these bursts it is possible to identify features associated with the propagation of S, P, and R waves, and these bursts can be interpreted as separate sources. They are called aftershocks. An attempt to view them as a signal generated by a single process evolving in space and time was made in Ref. 17 for the March 28, 1964 earthquake. The results are shown in Fig. 5. They permit drawing most of the foregoing conclusions, but there are two significant shortcomings. The first one is that the information is interpreted only for large delays relative to the main shock. The first aftershock is recorded only after 1 h 15 min. This is a very long delay; by this time, the first stage of the earthquake, together with all aftereffects, is over.

The second shortcoming is that the intermediate points are missed. This defect is especially significant for strong earthquakes that cause several faults to move. For this reason the signal must be interpreted in greater detail. Two possibilities were analyzed. The first one is the interpretation of separate phases of the oscillatory process and the second one is an extension of the concept of an aftershock.

An attempt to implement the first possibility was made in Ref. 9. On the basis of records from a large number of stations it was possible to correlate the maxima of the first seven oscillations of the P wave and to determine a 2-min segment of the trajectory. Further interpretation was found to be impossible. The trajectory cannot be traced up to the moment at which the side branches are formed, and even the onset of the tsunami focus formation cannot be found. These are difficulties of interpretating signals with a large number of oscillations. They are well known in the field of speech recognition based on an acoustic signal.[35] Mathematics provides two paths to the solution: the theory of signal detection when the signal is given by a nonstationary random process,[10,11] and successive regularization, when the signal is smoothed using different averaging times and a time interval is sought during which a stable interpretation is obtained.[36,37,40] These two methods complement one another. Detection theory suggests that the signal be represented not by its amplitude but rather by its instantaneous spectrum—the Wigner function (see Ref. 38); regularization proposes a criterion for selecting the time interval for averaging in order to construct the instantaneous spectrum. The type of result to be expected is obvious from the model experiment—a sequence of instantaneous point emitters.

Thus the quantity being interpreted is the instantaneous spectrum

$$A(\omega, t, R) = \int \overline{\xi\left(t+\frac{\tau}{2}\right)\xi\left(t-\frac{\tau}{2}\right)}\cos\omega\tau\, d\tau;$$

here ξ is the record of the signal. The instantaneous spectrum is a physical quantity. In the process of propagation it is transformed according to the laws of signal conversion:[39]

$$A(\omega, t, R) = \int K(\omega, t-t', R)\, A(\omega, t', 0)\, dt';$$

here $A(R)$ is the instantaneous spectrum at a distance R from the source, $A(0)$ is the instantaneous spectrum of the radiation, and K is the impulsive transfer function, which depends on the frequency ω and the distance R.

The instantaneous spectrum is employed in the analysis of seismic signals. In Ref. 13 it is constructed from the seismogram obtained in Makhachkala, and it is shown in Fig. 22 in the form of the lines $|A(\omega,t)| = \text{const}$.

The representation by means of the instantaneous spectrum is significantly simplified, if the signal has a quasiuniform structure, for example, it is represented in the form of a sequence of pulses of the same type with random delays θ_i and amplitudes A_i, i.e., $\xi(t) = \Sigma_i A_i \eta(t-\theta_i)$. We note that only such a representation is possible for reading a record of poor quality, when only the magnitudes and times of successive maxima and minima of the signal are determined. In this case the instantaneous spectrum factorizes, i.e., it can be represented as a product of only time-dependent and only frequency-dependent factors:

$$A(\omega, t) = C(\omega)\, B(t).$$

The magnitude of the temporal factor $B(t)$ does not depend on the structure of a separate pulse and is determined only by the repetition frequency $n(t)$ and the mean-square ampli-

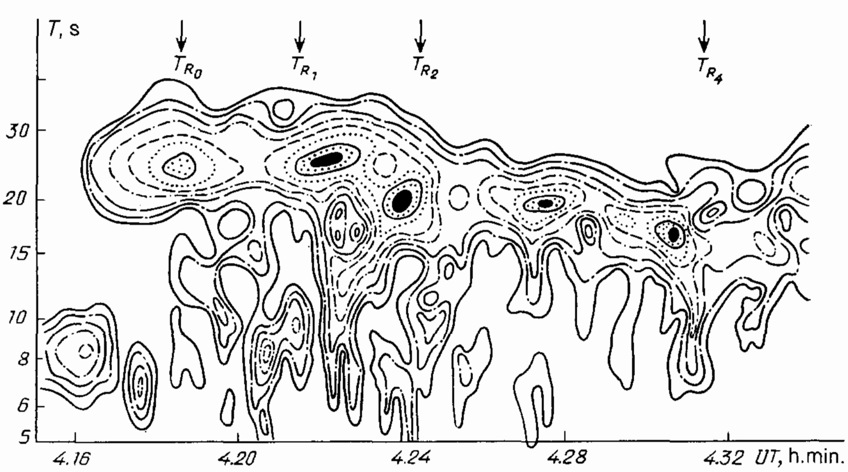

FIG. 22. SVAN diagram (instantaneous spectrum) of the SK record of the March 28, 1964 Alaskan earthquake. The regions of maximum values are colored black. The isolines are drawn every 1 dB.

tude $\overline{A^2}(t)$, i.e., $B(t) = n(t)\ \overline{A^2}(t)$.

This quantity for the first hour of the seismogram of the 1964 Alaskan earthquake is shown in Fig. 23. It is obvious that the analysis must be limited to interpretation of the bursts (series of maxima), which are the analogs of the aftershocks.

The problem of interpretation is to estimate the location of the sources and the excitation times of the successive maxima. For this, it is important to correlate uniquely the maxima recorded at different stations. If the propagating velocity of the wave is higher than the velocity of the source, the maxima at different points follow in the same order and the order number can serve as a distinguishing indicator. However there arise difficulties owing to the multiple channel nature of the propagation: the S wave of the delayed source can lead the R wave of the preceding source. The confusion can be eliminated by limiting the dynamic range and interpreting the records at large distances, when the amplitude of the Rayleigh waves is much greater than that of the other waves (see Fig. 23b). However this is not very convenient for solving prediction problems: Additional delays appear owing to propagation and the difficulty of transmission of information. The problem is best solved with the help of near-zone records.

In this case, to calculate the instantaneous spectrum the signal averaging time must be specially chosen:

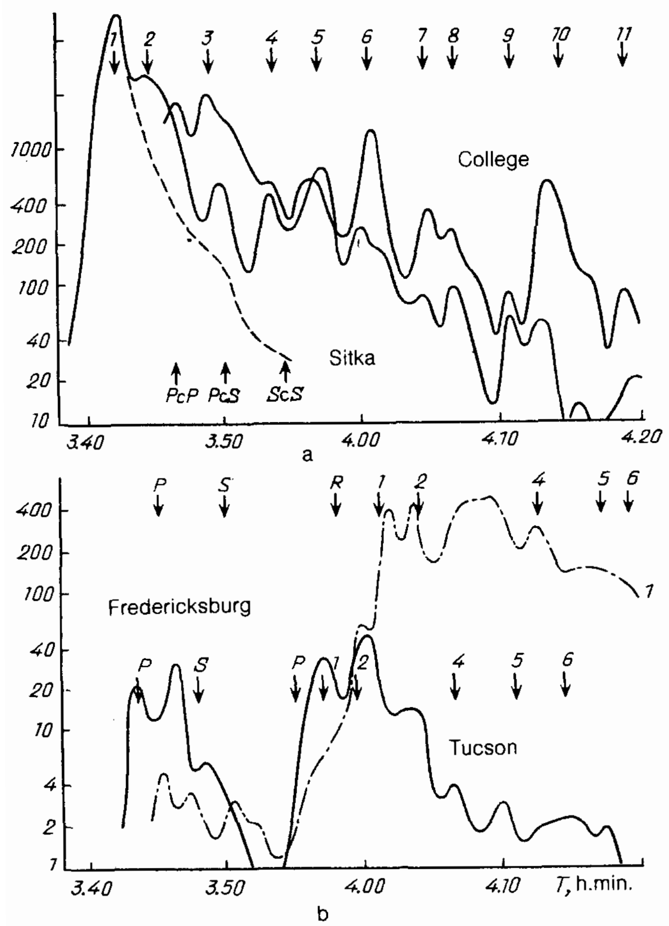

FIG. 23. Temporal factors of the instantaneous spectrum of the seismic signal for the March 28, 1964 Alaskan earthquake. a) Near zone. b) Far zone.

$$B_\theta(t) = \sum A_i^2(t)\,\frac{1}{\theta},$$
$$t - \frac{\theta}{2} < t_i < t + \frac{\theta}{2}.$$

This is a typical problem of regularization of the representation.[37] For long averaging times the quantity B_θ has only one maximum and the result is equivalent to a point-like representation of the source. For times that are too short there arises confusion, associated with the multiple-channel nature of the propagation, in the interpretation of the numbers of the bursts. A concrete choice can be made by analyzing specific records. In Ref. 13 records of distant aftershocks were used for this purpose. It follows from the analysis that for a 1-min averaging interval for signals emitted from distances of up to 1200 km the maxima associated with different propagation channels merge and the instantaneous spectrum of the aftershock is a unimodal curve; in addition, the position of the maximum propagates with a velocity of 3.2 km/s.

The temporal factor of the instantaneous spectrum of the seismic signal obtained for the March 28, 1964 earthquake with an averaging time of 1 min is shown in Fig. 23. One can see that 12 additional maxima are reconstructed between the first burst and the first aftershock; each maximum can be clearly identified from the records obtained at different stations. These data were employed to construct the trajectory shown in Fig. 11.

A very important question in using this method is the question of resolving the bursts in time. The averaging interval θ limits the possible resolution. An interval of 1 min is characteristic for records obtained at a distance of 1000 km. Such resolution is sufficient for interpreting the Alaskan earthquake, whose focus has a characteristic size of 700 km, so that the 5-km resolution provided by such an averaging interval is to some extent sufficient for obtaining additional information. For moderate earthquakes, however, when the characteristic size of the focus is about 100 km, this is not sufficient. This question requires further analysis. From the physical standpoint the time θ must be proportional to the distance from the source. If this is so, then analysis of small earthquakes requires a denser network of stations, whose distance from the source is not much greater than the length of the focus.

Some remarks concerning the signal record are in order. The requirements which the record must meet are largely determined by the aim of the measurements. At the present time the aim is to determine accurately the time of the first arrival, which is used to determine location. An example of such a record is shown in Fig. 24; this is not a specially selected example. From several tens of signals, obtained from the Center for Data on the Alaskan Earthquake, only one was found to be suitable for constructing a SVAN diagram. Such a record does not give the data required to construct the trajectory. The trajectory was reconstructed due to an accidental circumstance. It turns out that magnetometers react to a seismic signal. Magnitude 5 earthquakes can be clearly recorded from a distance of 1000 km with a sensitivity of 1 γ. In the process, shocks of magnitude 8 are observed without saturation and disruption of the record. Such a record makes it possible to determine the phase of the trajectory, and in the process frequency components with periods ranging from 10 to 70 s are employed for locating the

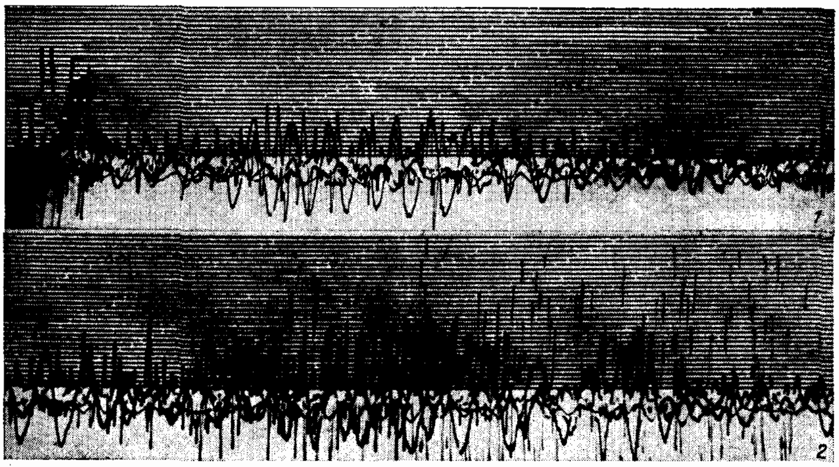

FIG. 24. Standard seismogram of the March 28, 1964 earthquakes (record made in Kirovabad). The spacing between the time markers is equal to 1 min; the time increases from right to left.

maxima. The main requirements are that the dynamic range must be large and the reverberations must be small. High-quality acoustic systems usually must meet both requirements, which apparently are the main requirements that must be met when organizing observations of signals with a large number of oscillations, interpreted as a nonstationary random process.

Thus the trajectory is a measurable quantity. The determination of the trajectory makes it possible to obtain quite detailed information about the evolution of the earthquake process. *Such information is useful for solving the problems* of providing earthquake warnings.

7. CONCLUSIONS

Progress in seismology is driven not only by scientific interests but also by public interests—organization of industrial and vital activities in seismically active regions. Earthquakes cause damage and kill people.

On the one hand, the model of an earthquake as a nearly instantaneous single-event process employed in the solution of practical problems, does not correspond to the physical picture of the phenomenon which evolves over several hours and in the process extends into progressively newer locations. On the other hand, this model does not provide the lead time and the extra space required for solving the earthquake-warning problem.

The representation of an earthquake by a moving source emitting random oscillations is a more detailed model, which can be used for organizing earthquake warnings.

Providing an earthquake warning reduces to solving three main questions: 1) How often and with what intensity do earthquakes occur in a given location (long-term forecast; the purpose is to develop building codes and rules for living in such a location)? 2) Where, when, and with what intensity will destruction begin as a result of an earthquake (short-term forecast; the purpose is to develop an alarm signal)? 3) What will be destroyed in a given earthquake and what more can be expected from it (prediction of aftereffects of an earthquake; the purpose is to develop additional alarms, such as a tsunami alarm, and plans for dealing with the aftereffects)?

Seismic and tsunami zoning are concerned with the solution of the first question. The main source of information are historical data on past earthquakes (Fig. 25). For each earthquake empirical formulas are employed to calculate the intensity of the vibrations as a function of the maximum acceleration of the seismic vibrations. The result of the calculations for the March 28, 1964 earthquake in Prince William Sound is shown in Fig. 4. The maximum possible intensity is determined by using all events; this intensity characterizes the earthquake danger. This is a continuous function of the distance from the zone of maximum earthquakes. The actual data show that the situation is not this simple, since the magnitude is a rapidly varying function. An *example is the earthquake in Armenia. It was found that* windows in houses located several kilometers from the zone of the disaster were not broken.[41] This phenomenon is usually attributed to the quality of the construction, but this is merely a concession to the tradition of seeking the guilty

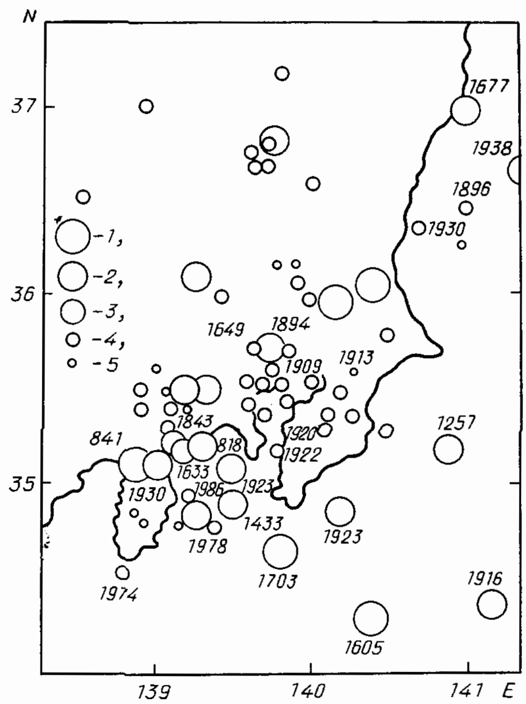

FIG. 25. Map of earthquakes in the region of Tohoku (Japan). *1*) Magnitude greater than 8, *2*) magnitude greater than 7.5, *3*) magnitude greater than 7, *4*) magnitude greater than 6.5, *5*) magnitude greater than 6.0.

party. More objective data can be obtained by analyzing the leveling of the forest along the Fairweather fault by the Alaskan earthquake of July 10, 1958;[22] it was found that the zone of maximum damage is concentrated in a 100-m neighborhood of some line running parallel to the axis of the fault. In some locations the width of the zone increases to 1-2 km (on lake shores). For this reason the epicenter and the magnitude give a too general representation, as a result of which the effects localized in small regions are assigned to a large region. This generalization leads to harmful consequences. At the last seismology conference (Vladivostok, 1989) it was reported how the population fled Kamchatka as a result of the prediction of an earthquake.[41] Judging from the size of the region of destruction it is obvious that one should run not onto the mainland, but rather into a neighboring block, it being very likely that if a house withstood the earthquakes of 1952 and 1971, which destroyed everything at locations where damage should occur, then the house is located in a safe zone. The main shortcoming of this representation is that the principal destructive factors are not taken into account correctly; these should include not only the maximum accelerations, but also deformations of the foundations. The latter are correlated with locations of mobile faults. For this reason, earthquake zoning must be based on a representation of an earthquake which contains all faults along which movements have occurred. The trajectory contains this information.

The second question of the earthquake-warning problem is the question of providing an early warning of an earthquake. Since in the simplest representation the main shock is simultaneously a signal and a source of damage, this concept is not conducive to attempts to employ the seismic signal for prediction. Some indirect data on the character of the development of seismic activity in the past make it possible to formulate (not very convincingly) predictions, whose accuracy is determined by the rate of change of seismic activity and does not exceed several years. Such a prediction, as experience in Japan[42] and now also Kamchatka shows, does more harm than good. For this reason, all searches for methods for making timely and accurate predictions are based on the study of phenomena of a different nature—phenomena which vary over shorter times. The main phenomenon are displacements of the earth's surface, which in some locations undergo variations with a characteristic duration of several days, and the production rate of springs in regions closest to the focus. The obtained results are tied to specific sections of a location.[42]

From our point of view, the simplified representation of an earthquake does not adequately utilize the possibility of damage prediction. The latter, as a rule, is delayed by at least several minutes relative to the main shock. Sometimes this delay is several hours. This circumstance is employed by local inhabitants of seismically active regions, where earthquakes do not kill as many people as did, for example, the Armenian earthquake. In Ref. 43 it is pointed out that even in the Armenian earthquake the destructive shock was the second one, which was delayed by several minutes, and the earthquake became a killer because people did not make use of this extra time. Analysis of the trajectory of an earthquake reveals the character of the evolution of the earthquake already at the leader phase and it makes it possible to determine from the intermediate maxima the position of dangerous faults, i.e., to predict by several minutes the most important aftereffects.

Tracing the successive stages of an earthquake makes it possible to evaluate the situation and to predict by ten minutes each new motion, i.e., with a short lead time, but accurately enough to predict damage development.

The third question is the prediction of dangerous aftereffects. The most interesting aftereffects are tsunamis, whose influence zone is much greater than the region of damage and in some cases (the Chile tsunami of May 20, 1960) extends over tens of thousands of kilometers.[44] There exists a worldwide tsunami warning service. The main station is located in the Hawaiian Islands. The service provides quite accurate warnings of the danger of transoceanic tsunamis; both the times and amplitudes of the waves on coastal sections far from the source are determined. Such predictions are based primarily on the tsunami observations at points close to the focus. In this system, however, there are no reliable methods for predicting tsunamis in sections close to the source; this became a subject of discussion at the 12th session of the JOC.[45] The six largest tsunamis of the last decade occurred in the Philippines on August 17, 1976, Indonesia on August 19, 1977, Indonesia July 18, 1979, Papua New Guinea on September 12, 1979, Colombia on December 17, 1979, and Japan on May 26, 1983 and they were practically unpredictable and caused great loss of life. For this reason the worldwide service must be supplemented by regional services, which must give a prediction of tsunamis from earthquakes which occur very close to shore. Such services exist in Alaska, in Japan for six different regions, and in the Soviet Union. The work performed by the service depends on measurements of seismic signals, from which the epicenter, the depth, and the magnitude of the earthquake are estimated. If the epicenter of the earthquake is located underneath the ocean bottom, if the depth of the earthquake does not exceed 150 km, and if the magnitude of the earthquake is not less than 7, then a tsunami alarm is sounded. On the basis of this alarm, in particular, fish processing combines cease operations and people living along the coast leave their homes and go to higher ground. The arrival time of the wave is estimated from the time and the epicenter of the earthquake.

Attempts are being made to supplement the system with extended cable tsunami detectors, which would make the prediction unique and accurate. The warning is given almost everywhere.

The main drawback of the present system is that it generates a large number of false alarms. Practically all predictions made over the last 20 years were false alarms: either the tsunami did not exceed 1 m in height and the water level did not exceed the maximum high tide or a wave which sea-level gauges could record did not occur at all. The alarms themselves, which continued for quite a long time, even after it became obvious that there is no wave (the time exceeded the propagation time of the wave from the epicenter to the point of observation), caused much trouble and losses of tens and hundreds of thousands of rubles. In addition, it should be noted that an alarm is sounded over the entire region at once, and the less the danger, the farther away from the earthquake the point is, the longer the waiting period is, and the worse the aftereffects are. As a result the public distrusts tsunami warnings.

The second shortcoming is that some warnings are missed. In practice this happens only as a result of technical errors (the case of the 1983 tsunami in the Sea of Japan, a warning was given for the Kurile Islands, but the wave was observed along the sea coast). The principles on which the system is based can themselves lead to such errors. This happened, for example, in the case of the March 28, 1964 earthquake in Alaska. The epicenter of this earthquake was located on land, and the closest sea shore was the shoreline of Prince William Sound. According to the prediction based on the point-source model either an alarm should not have been sounded at all or it should have been sounded only for the shoreline of Prince William Sound. At that time the tsunami from this earthquake struck not only the closest shores (Kodiak Island, Kenai Peninsula), but loss of life also occurred in Crescent City (California) and the distant Chilean coast.

The third shortcoming is that the arrival time of the wave is not correctly estimated. Figure 26 shows a histogram of the arrival time deviations from the estimates based on the model—from the propagation time of the wave from the epicenter to the point of observation for the case of the Chilean tsunami. I deviated here from presenting data pertaining to only the Alaskan earthquake because in the latter case the epicenter was subterranean and theoretically the time cannot be calculated at all. From the histogram one can see large discrepancies (up to 1 h and longer), and in addition a) the wave, as a rule, arrives earlier than predicted and b) the discrepancies are not related with the quality of the calculations of the propagation time; large deviations are observed for both large and comparatively small distances from the epicenter, and the magnitudes of the deviations are a continuous function of the geographic coordinate or, more accurately, the direction of propagation of the wave, i.e., it is obvious that at least for regional warnings such an estimate is virtually useless; the error of the estimate is equal to the magnitude of the delay itself.

In some articles it is mentioned that a short lead time sometimes makes prediction of the wave useless. But in making such a statement it is forgotten that the prediction refers to the arrival time of the wavefront and not the wave maximum. In actuality, sometimes a tsunami arrives as a bore and the maximum positive amplitude (inundation) arrives together with the front, but this does not always happen. In many cases (Kamchatka tsunami 1952 in the northern Kurile Islands) the wave starts with an ebb, but it can also start with a slow rising of the water level, as happened in the 1964 Alaskan tsunami, when against a slowly rising background a

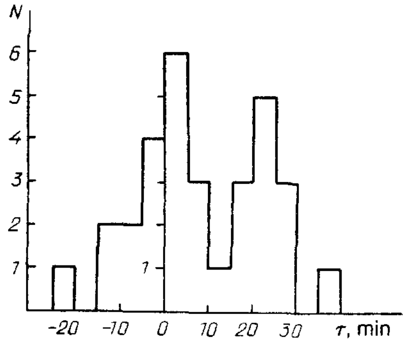

FIG. 26. Distribution of deviations of the estimate of the wave arrival time from the true value for the May 20, 1960 Chilean earthquake.

large positive wave arrived only 15 min later (Sitka). For this reason, in many cases analysis of the structure of the wavefront can increase the time available for taking reasonable precautions against the tsunami. The model does not give this lead time. To obtain the extra time it is necessary to predict the shape of the frontal wave.

The local population criticizes most the fact that an all-clear signal is not given. Generally speaking, in accordance with doctrine, the process occurs instantaneously, and if at that instant nothing has happened, i.e., after the seismic signal a wave has not arrived in the corresponding time, then, one would think, that an all-clear signal would be given. However this is not done and correctly so, because the process evolves in time and the wave can be generated much later than the so-called main shock. It has happened that the arrival of the wave was delayed by several hours (Seldovia, Prince William Sound earthquake of 1964, and Crescent City (California), Alaskan earthquake of 1964). In Crescent City, in particular, a man was killed when he returned home too soon after the first two waves receded. But the model does not make it possible to interpret information contained in the flux of seismic signals, and for this reason an all-clear signal is not scientifically justified; it is given quite arbitrarily and, as a rule, after a long delay.

Thus it is obvious that the model of an earthquake as a single-event process which evolves over a time of about 100 s is clearly inadequate for resolving the main earthquake-warning problems. In order to develop such a model the physical process—the destruction caused by the earthquake—must be investigated in greater detail and the seismic signals that are generated in the process must be carefully analyzed.

Tracing the trajectory of an earthquake makes possible significant progress toward the solution of the questions enumerated above.

Question of false alarms. The number of false alarms can be significantly reduced on the basis of two properties of the process which are revealed by analyzing the trajectory. The first property is the presence of an oscillatory phase, an indication of the opening of a fault, after which motion of the fragments and generation of an intense wave start. The second property is the intensity of and the direction toward the focus and the velocity of the process along the axis of the rupture plane. Estimation of these characteristics makes it possible to estimate the region where the wave will strike and to limit significantly the territory for which the alarm is sounded.

Question of missing of signals for subterranean earthquakes. Observation of the trajectory gives a scientific basis for the solution of this question, since it makes it possible to observe when and where the process emerges from beneath the ocean bottom.

Question of arrival time estimation. The tsunami focus is estimated from the trajectory with the same accuracy with which the focus is estimated from near-zone observations of the wave.

Question of the prediction of the appearance of an intense wave. The solution of the question of the generation of an intense wave depends on the observation of the start of the transition of the process from the leader phase to the rupture formation phase. This information is contained in the trajectory.

Question of an all-clear signal. This is a question of estimating the time when the process responsible for generating the tsunami has stopped. The information required to solve this question is contained in the trajectory of the process. It is not easy to interpret. It is of a two-step character. The position of the faults that participate in the process is estimated from an analysis of the leader phase; analysis of the stages makes it possible to determine which faults have already opened. If all disturbed faults are open, then the wave generation process is close to completion. In the case of the March 28, 1964 earthquake there were six transverse faults and the low-frequency component of the tsunami had six principal maxima.

Thus making the representation of an earthquake more complicated by introducing a moving source opens up extensive possibilities for earthquake prediction.

The same representation, however, makes it possible to analyze in greater detail past earthquakes. It also raises the problem of the interrelationship and interdependence of different processes occurring in an earthquake. To solve this problem the methods employed for interpreting seismic signals must first be improved unfettered by the ideological shackles of official science and by not permitting the measurements to be perverted so as to favor existing dogmas.

[1] G. A. Eiby, Earthquakes, Van Nostrand Reinhold Co., N. J., 1980 [Russian translation, Nauka, M., 1982, p. 263].
[2] N. N. Scott and W. K. Cloud, The Prince William Sound Earthquake of March 1964 and Aftershocks, US Department of Commerce, Washington, 1969, Vol. 2, Part B, p. 5.
[3] Tsunami: Their Science and Engineering, TERRAPUB, Tokyo, 1983.
[4] *Seismic Zoning of the USSR* [in Russian], Nauka, M., 1980.
[5] J. Rice in *New Ideas in Science Abroad. Series in Mechanics* [Russ. transl., Mir, M., 1982, p. 217.
[6] A. Ben-Menachem, Bull. Seismol. Soc. Am. **51**, 401 (1961).
[7] A. A. Gusev, Vulkanologiya i Seismologiya, No. 1, 3 (1984).
[8] L. Ruff and H. Kanamori, Phys. Earth Planet. Inter. **31**, 202 (1983).
[9] M. Wyss and J. N. Brune, Bull. Seismol. Soc. Am. **57**, 1017 (1967).
[10] C. Helstrom, *Statistical Theory of Signal Detection*, Pergamon Press, N. Y., 1968 [Russ. transl., Inostr. lit., M., 1963, p. 430].
[11] V. V. Ivanov and L. C. Chudnovskiĭ, *Impulsive Electromagnetic Fields of Fast Processes and Measurement of Their Parameters* [in Russian], Atomizdat, M., (1978).
[12] V. V. Ivanov and O. I. Garder, Dokl. Akad. Nauk SSSR **283**, 1149 (1985) [Dokl. Earth Sci. (1985)].
[13] V. V. Ivanov and N. P. Konstantinova, Vulkanologiya i Seismologiya, No. 5, 64 (1988).
[14] V. V. Ivanov, O. I. Garder, A A. Kharlamov, and L. S. Chudnovskii, *Natural Catastrophes and Natural Disasters in the Far East* [in Russian], Far-East Branch of the Academy of Sciences of the USSR, Vladivostok, 1990, Vol. 1, p. 48.
[15] *Fracture Mechanics: Fast Fracture, Stopping of Cracks* [Russ. transl., Mir, M., 1981.]
[16] A. V. Vikulin and I. P. Chernobaĭ, *Dynamic Processes in Discrete Geophysical Systems* [in Russian], Far Eastern Branch, Acad. Sci. USSR, Vladivostok, 1986, p. 58.
[17] S. T. Algermissen, W. A. Reinhart, R. W. Sherburne, and W. H. Dellinger in Ref. 2, p. 79.
[18] L. M. Hastie and J. C. Savage, Bull. Seismol. Soc. Am. **60**, 1389 (1970).
[19] *Handbook of Geophysics: Atmospheric Electricity* [in Russian], Nauka, M., 1965, pp. 209–229.
[20] T. Hatori, in *Tsunamis in the Pacific Ocean*, Honolulu, 1970, p. 60.
[21] S. Satake and H. Kanamori, Tsunami '89: Abstracts, Novosibirsk, 1989, p. 45.
[22] D. Tocher, Bull. Seismol. Soc. Am. **50**, 217 (1960).
[23] G. A. Pararas-Carajannis, Pacific Sci. **21**, 301 (1967).
[24] L. N. Sretenskiĭ, *Theory of Wave Motions in Liquids* [in Russian], Nauka, M., 1977, p. 815.
[25] K. Abbe and H. Ishii, J. Oceanograph. Soc. Jpn. **43**, 169 (1987).
[26] V. V. Ivanov in: Ref. 14, p. 121.
[27] Tsunami Travel Time Charts for Use in the Tsunami Warning System, US Department of Commerce, Washington, 1971.
[28] The Prince William Sound Earthquake of March 1964 and Aftershocks, US Department of Commerce, Washington, 1969, Vol. 3, p. 161.
[29] V. V. Ivanov, Izv. Akad. Nauk SSSR, Ser. Fiz. Zemli, No. 1, 88 (1988) [Izv. Acad. Sci. USSR Physics of the Solid Earth, **24**, 63 (1988)].
[30] L. D. Landau and E. M. Lifshitz, Theory of Elasticity, Pergamon Press, N. Y., 1970 [Russ. original, Fizmatgiz, M., 1960, p. 400].
[31] V. F. Vyalykh in *Tsunami Conference* [in Russian], Gor'kiĭ, 1984, p. 27.
[32] J. B. Small and L. C. Wharton in: Ref. 28, p. 21.
[33] E. J. Parkin, *ibid.*, p. 35.
[34] A. J. Pope, *ibid.*, p. 99.
[35] J. Flanagan, *Speech Analysis, Synthesis, and Perception, Academic Press*, N. Y., 1965 [Russ. transl., Svyaz', M., 1968].
[36] A. N. Tikhonov, Dokl. Akad. Nauk SSSR **151**, 49 (1963) [Sov. Math. Dokl. **4**, (1963)].
[37] V. Ya. Arsenin and V. V. Ivanov, Radiotekh. Elektron. **14**, 167 (1967).
[38] R. Feynman, *Statistical Mechanics*, W. A. Benjamin, Reading, MA, 1972 [Russ. transl., Mir, M., 1978, p. 407].
[39] V. V. Ivanov and O. I. Garder, Izv. Akad. Nauk SSSR, Fiz. Zemli, No. 12, 72 (1987). [Izv. Acad. Sci. USSR, Physics of the Solid Earth, **23**, 1022 (1987)].
[40] V. Ya. Arsenin and V. V. Ivanov, Dokl. Akad. Nauk SSSR **182**, 9 (1968) [Sov. Math. Dokl. **9**, 1067 (1968)].
[41] M. A. Klyachko, *Abstracts of Reports at the Regional Session of MSSS* [in Russian], Far-East Branch of the Academy of Sciences of the USSR, Vladivostok, 1989.
[42] K. Mogi, *Earthquake Prediction*, Academic Press, N. Y., 1985 [Russ. transl., Mir, M., 1988, p. 382].
[43] R. A. Kerr, Science, January 13 (1989).
[44] The Chilean Tsunami of May 24, 1960 as Observed Along the Coast of Japan, The Committee of Field Investigation of the Chilean Tsunami of 1960, Tokyo (1961).
[45] 12th Session of the IOC International Coordination Group for the Tsunami Warning System in the Pacific, August 7–10, 1989, Joint Report, Novosibirsk (1989).

Translated by M. E. Alferieff